

Pittsburg State University

## Pittsburg State University Digital Commons

---

Electronic Theses & Dissertations

---

12-2013

### Structural characterization of super-acid oligomerized fatty esters.

Esam Allehyani  
*Pittsburg State University*

Follow this and additional works at: <https://digitalcommons.pittstate.edu/etd>

 Part of the [Chemical Engineering Commons](#), and the [Chemistry Commons](#)

---

#### Recommended Citation

Allehyani, Esam, "Structural characterization of super-acid oligomerized fatty esters." (2013). *Electronic Theses & Dissertations*. 114.

<https://digitalcommons.pittstate.edu/etd/114>

This Thesis is brought to you for free and open access by Pittsburg State University Digital Commons. It has been accepted for inclusion in Electronic Theses & Dissertations by an authorized administrator of Pittsburg State University Digital Commons. For more information, please contact [digitalcommons@pittstate.edu](mailto:digitalcommons@pittstate.edu).

STRUCTURAL CHARACTERIZATION OF SUPER-ACID OLIGOMERIZED FATTY  
ESTERS

A Thesis Submitted to the Graduate School  
In Partial Fulfillment of the Requirements  
For The Degree of Master of Science

Esam Allehyani

Pittsburg State University

Pittsburg, Kansas

December 2013

STRUCTURAL CHARACTERIZATION OF SUPER-ACID OLIGOMERIZED FATTY  
ESTERS

Esam Allehyani

APPROVED:

Thesis Advisor

\_\_\_\_\_

Dr. Madhusudhan Srinivasan, KPRC

Committee Member

\_\_\_\_\_

Dr. Khamis Siam, Chemistry Department

Committee Member

\_\_\_\_\_

Dr. William M. Shirley, Chemistry Department

Committee Member

\_\_\_\_\_

Dr. Charles Neef, Chemistry Department

## **ACKNOWLEDGEMENTS**

I would like to express my sincere gratitude to many people who help and support me all the time. I would express especial thanks to my lovely parents my father Saleh and my mother Saleha. Also, I would like to thank my amazing wife for her personal support and great patience at all times and to my newborn son Saleh. In addition, I would like to thank all my brothers Ayman, Husam, Ahmed, and Feras.

I would like to express especial thank to my sponsor Umm Alqura University that gave me the opportunity to continue my studies and my knowledge.

I would like to thank my advisor Dr. Madhu Srinivasan, all my Committee members, and my faculty. In addition, I would like to thank my brothers Ahmed Alzharani and Esam Alqurashi, all my nice friends, and my classmates.

# STRUCTURAL CHARACTERIZATION OF SUPER-ACID OLIGOMERIZED FATTY ESTERS

An Abstract of a Thesis By

Esam Allehyani

Fatty acid methyl esters can be oligomerized with very strong acid catalysts - superacids such as tetrafluoroboric or triflic acid with formation of dimer and trimer fatty acids at much lower temperature, such as 80-90 °C, than what is used presently. Insight into the reaction of polymerization of fatty esters/ acids can be obtained by structural characterization. This would determine the properties of the oligomeric products and their ability to substitute currently used materials. It was presumed that dimer fatty, trimer fatty acid esters, and oligomeric fatty acid esters are produced by polymerization of fatty acid methyl esters by a cyclization reaction involving the double bonds of the fatty acid chain.

The proposed reaction of fatty acid methyl ester and fatty acid were studied in two different factors: the effect of catalyst concentrations and temperature. It was found that increasing the concentration of the catalyst increased the formation of dimer and the other oligomers of methyl soyate, while, oleic acid showed formation of estolides and lactones. Furthermore, it was found that increasing the temperatures of methyl soyate increased the formation of the dimer and the other oligomers of methyl soyate, whereas, oleic acid showed a decrease in the formation of estolides and lactones.

# Table of Contents

CHAPTER	PAGE
<b>CHAPTER I</b>	<b>1</b>
1. INTRODUCTION:	1
1.1 <i>Background and literature review:</i>	3
1.2 <i>Cationic polymerization:</i>	5
1.3 <i>Project rationale:</i>	6
2. EXPERIMENTAL:	9
2.1 <i>Materials:</i>	9
2.2 <i>Instrumentation:</i>	9
2.3 <i>Methods:</i>	10
2.3.1 <i>Transesterification:</i>	10
2.3.2 <i>Oligomerization:</i>	10
<b>CHAPTER III</b>	<b>12</b>
3. RESULTS AND DISCUSSION:	12
3.1 <i>The Effect of Catalyst Concentration:</i>	12
3.1.1 <i>Gel Permeation Chromatography (GPC):</i>	13
3.1.2 <i>Fourier Transform Infrared Spectroscopy (FTIR):</i>	15
3.1.3 <i>Nuclear Magnetic Resonance (NMR):</i>	16
3.2 <i>The Effect of Temperature:</i>	23
3.2.1 <i>Gel Permeation Chromatography (GPC):</i>	24
3.2.2 <i>Fourier Transform Infrared Spectroscopy (FTIR):</i>	26
3.2.3 <i>Nuclear Magnetic Resonance (NMR):</i>	28
<b>CHAPTER IV</b>	<b>38</b>
4. CONCLUSIONS:	38
<b>REFERENCES</b>	<b>40</b>
<b>APPENDIX</b>	<b>43</b>

## List of Tables

TABLE	PAGE
Table 1. Composition of Vegetable oil <sup>3</sup> .....	2
Table 2. Calculations of Monomer: Initiator ([M]/ [I]) and double bond: Initiator ratios of Methyl Soyate samples .....	11
Table 3. Calculations of Monomer: Catalyst ([M]/ [I]) and double bond: Catalyst ratios of Oleic acid samples .....	11
Table 4. Calculation of the yield of Methyl soyate and Oleic acid after filtration .....	12
Table 5. Mw of MS oligomerized samples from GPC .....	14
Table 6. Mw of OA oligomerized samples from GPC .....	15
Table 7. Double bonds reduction of MS samples .....	17
Table 8. Double bonds reduction of Oleic acid samples .....	21
Table 9. Calculation the yield of Methyl soyate and Oleic acid after filtration.....	23
Table 10. Mw of MS oligomerized samples from GPC .....	25
Table 11. Mw of OA oligomerized samples from GPC .....	26
Table 12. Double bonds reduction of MS samples in different temperatures .....	29
Table 13. Double bonds reduction of Oleic acid samples .....	34
Table 14. Acid value and Iodine value of MS and OA samples .....	37
Table 15. Estolides yield of Oleic Acid .....	37

## List of Figures

FIGURE	PAGE
Figure 1. Structure of Oleic acid.....	2
Figure 2. Proposed reaction of dimer and trimer fatty esters.....	7
Figure 3. Formation of estolides and lactones from fatty acids.....	8
Figure 4. GPC trace of MS oligomerized samples.....	13
Figure 5. GPC trace of OA oligomerized samples.....	14
Figure 6. FTIR spectra of MS-1, MS-3, and MS-5 samples.....	15
Figure 7. FTIR spectra of OA-1, OA-3, and OA-5 samples.....	16
Figure 8. <sup>1</sup> H NMR spectra (a) MS starting material, (b) MS-5 oligomerized sample.....	18
Figure 9. <sup>13</sup> C NMR spectra (a) MS starting material (b) MS-5 oligomerized sample ....	19
Figure 10. <sup>1</sup> H NMR spectrum of (a) OA starting material (b) OA-5 oligomerized sample.....	20
Figure 11. <sup>13</sup> C NMR spectrum of (a) OA starting material (b) OA-5 oligomerized sample.....	22
Figure 12. GPC trace of MS-5 oligomerized samples at different temperature.....	24
Figure 13. GPC trace of OA oligomerized samples at different temperature.....	25
Figure 14. FTIR spectrum of MS-5 oligomerized samples at different temperatures.....	27
Figure 15. FTIR spectrum of OA-5 oligomerized samples at different temperatures.....	28
Figure 16. <sup>1</sup> H NMR spectra (a) MS starting material, (b) MS-5-90C oligomerized sample.....	30
Figure 17. <sup>13</sup> C NMR spectra (a) MS starting material (b) MS-5-90C oligomerized sample.....	31
Figure 18. <sup>1</sup> H NMR spectra of (a) OA starting material (b) OA-5-90C oligomerized sample.....	32
Figure 19. <sup>1</sup> H NMR spectrum OA-5-130C oligomerized sample.....	33
Figure 20. <sup>13</sup> C NMR spectra of (a) OA starting material (b) OA-5-90C oligomerized sample.....	35
Figure 21. <sup>13</sup> C NMR spectrum of OA-5-130C oligomerized sample.....	36



## **List of symbols and abbreviations**

FAME – fatty acid methyl ester

SOME – soybean methyl ester

HPLC – high performance liquid chromatography

ME – methyl ester

KPRC – Kansas Polymer Research Center- Pittsburg, KS

OA – oleic acid

MS – methyl soyate

MSSM – methyl soyate starting material

OASM – oleic acid starting material

# Chapter I

## 1. Introduction:

Vegetable oils are being explored as potential alternative sources to petroleum due to their economic and environmental importance.<sup>1,2</sup> They are obtained from plants in nature mainly derived from seeds and nuts.<sup>3</sup> Vegetable oil is generally applied to the oils that are in liquid form at ambient temperature, while the ones that are solid in nature are usually called vegetable fats. The main constituents of the vegetable oils are triglycerides.<sup>4</sup> They are widely used in the industrial sphere and can be extracted via mechanical extraction or solvent extraction.<sup>5,6</sup>

The importance of vegetable oil use is significant, especially with food shortages and cruelty-free food tendencies in the world. Thus, they are the substitutes for animal fat in cooking, cosmetics, fuel, and other uses of chemical products in industry and households. Current studies and use of oil in creating bio-fuel can contribute to sustainable agricultural businesses as well as clean energy. There is also a social movement globally for green production and consumption. Ecologically conscious consumers will want more choices and this desire will drive the research and development of materials from vegetable oils and biodiversity based food production.<sup>7</sup>

Fatty acids are classified as aliphatic monocarboxylic acids extracted from or inherent in esterified condition in vegetable oil. Fatty acids in nature normally have a tail of 4 to 28 carbons, which are mostly even-numbered and unbranched. They can be either saturated or unsaturated.<sup>8,9</sup> Saturated oils are, in chemical terms, a composite of a chain

of carbon atoms linked by single bonds, such as palmitic acid and stearic. Unsaturated oils are a chemical composite with carbon-carbon double bonds such as oleic acid (Figure 1), linoleic acid, and linolenic acid.

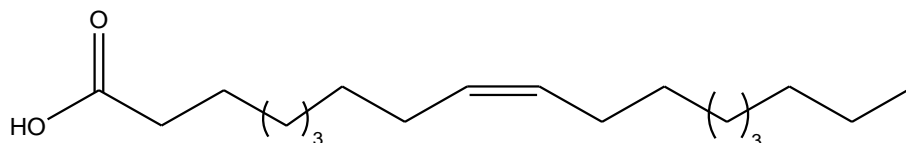


**Figure 1. Structure of Oleic acid**

**Table 1. Composition of Vegetable oil<sup>3</sup>**

<b>Fatty acid</b>		<b>Soybean</b>	<b>Canola</b>	<b>Cottonseed</b>	<b>Sunflower</b>	<b>Peanut</b>
Palmitic	16:0	11	4	25	7	12
Stearic	18:0	4	2	2	5	3
Oleic	18:1	23	64	18	19	47
Linoleic	18:2	53	19	53	68	31
Linolenic	18:3	8	9	0.3	1	-

The quantity of unsaturation in a fatty acid in vegetable oil can be determined by its iodine number. Iodine value is a mass of iodine in grams that is consumed by 100 grams of a chemical substance. The higher the iodine number, the higher the unsaturation is, as more C=C bonds are coherent in the oil. For instance, peanut oil is more saturated, which makes it useful for soap production (Table 1). As opposed, linseed oil is unsaturated, which makes it a drying oil, suitable for oil paints production.<sup>10</sup>

Drying oils absorb oxygen from the air and therefore can transform into plastic and resin-like substances. Drying oil has an iodine value greater than 140. They can be used in production of paints, varnishes, where addition of such oil to substance, after

being exposed to the air, lets it form a thin but very strong layer for example, linseed oil. Non-drying oils do not solidify upon drying and can be used in cosmetics, soaps, candle production, and as supporting components in various industrial processes. Semi-drying oils stand between drying and non-drying oils with an iodine value between 125-140, and although they absorb oxygen to some extent, they do not transform completely for example, soybean and corn oils. Non-drying oil does not absorb oxygen from the air and the iodine value is less than 125.<sup>11</sup>

Dimer acids are dicarboxylic acids derived from unsaturated fatty acids obtained from vegetable oil by the process of dimerization, mainly using clay catalysts. Dimer acids are not toxic and are used for polyamide resins and polyamide hot temperature melts and fuel additives. It is a light yellow or yellow viscous transparent liquid. Trimer acid is similar to dimer acid but its molecule consists of three fatty acid molecules.

Triglyceride oils have a great significance as a product for protective and decorative organic coating because they are able to polymerize, cross-link, and dry after their application to the surface and dry to form adherent and tough coating. For this purpose, drying oils undergo the process of thermal polymerization and air blowing. For instance, in preparation of air-blown linseed oil, air is passed through heated oil while the temperature is controlled.<sup>12</sup> Cationic polymerization is a chain reaction used to grow polymers by using the reaction of monomers and reactive side of polymers, specifically by ions, where the kinetic-chain carriers are cations.<sup>13</sup>

### **1.1 Background and literature review:**

Polymerization of oil has been reviewed in different sources of literature, since it has various theoretical aspects as well as the practical applications. Ionescu and Petrović

discussed the process of cationic polymerization of soybean oil. They showed that polymerization of oil can be carried out at the temperature of 90 °C with superacid. Furthermore, it is stated that their process of oligomerized soybeans have great economic importance than thermal polymerization, which can be conducted with lower energetic expenses.<sup>14</sup> They proposed a mechanism for soybean oil cationic polymerization via a Diels-Alder or ene reaction.

The researchers received a patent for the method of cationic polymerization of unsaturated biological oils.<sup>15</sup> The reaction is stated to be carried out via the double bonds, which are initiated by the superacids. The resulting oligomerized oils have about 10-200 times more viscosity than the initial soybean oil, whereas, decreasing the unsaturation as compared to the initial soybean oil.

Larock et al investigated the cationic copolymerization of soybean oil with divinylbenzene comonomer by using boron trifluoride diethyl etherate as an initiator at different temperatures: room temperature, 60 °C, and 100 °C.<sup>16</sup> He found that the oligomerized soybean with divinylbenzene is thermally stable and can provide a wide range between rubbers to thermosets. The important factors for the structure of polymers depended on stoichiometry, source of soybean oil, and initiator. It was also found that increasing the concentration of divinylbenzene increased the yield of the crosslinked polymers.

The cationic polymerization of soybean oil creating low molecular weight derivatives from soy materials with boron trifluoride diethyl etherate as an initiator in 100- 140 °C and 110 bar.<sup>17</sup> The investigation considered the impacts of the main constituents of the experiment, such as polymerization temperature, initiator amount, and

pressure of the carbon dioxide. It was concluded that increase temperature of the polymerization as well as usage of more initiator lead to higher molecular weights in the polymers. The soy materials that were produced can be used in the variety of the industrial applications where these properties are necessary.

Numerous patents have reported materials derived from the polymerization of the biological oils, conjugated biological oils, and metathesized or cometathesized biological oils.<sup>18</sup> In addition, a large number of patents have reported materials derived from biological oils such as soybean oil, tung oil, and fish oil. They provide plastics and thermosets from variable renewable resources such as biological oils with the process of oligomerized these oils in presence of Lewis-acid catalyzed. The number of patents illustrates the practical implementation of different industrial materials, for example rubbers, elastomers, and plastics.

Apart from the soybeans, other plants can be used for the production of the dimer acids and dimer esters.<sup>19</sup> The researcher's state that dimer acids can be produced from a clay-catalyzed reaction from the meadowfoam alternative crop. Dimer acids that are produced from plants are used primarily for the cosmetic or medical purposes, and have a high viscosity that was compatible with commercial dimer esters. It has been reported that dimer acids and dimer esters can have the properties that are comparatively equal with those of the commercial representatives.

## **1.2 Cationic polymerization:**

Polymerization can be divided into two types: chain-growth and step-growth polymerization. Cationic polymerization is the chain-growth type of polymerization. In the cationic polymerization, the initiator is cationic and it transfers the charge to the

monomer in reaction. Cationic polymerization of biological oils can occur in the presence of superacids. The polymerization of vegetable oils has been proposed to proceed through an ene mechanism.<sup>20</sup> The crosslinking of soybean oil via an ene reactions in the soybean oil was proposed to occur when it diethyl azodicarboxylate at room temperature. Another possible reaction of soybean oils is a Diels-Alder reaction.

### **1.3 Project rationale:**

The proposed reaction (Figure 2) will be investigated via a cationic oligomerization using a superacid. Analysis of the methyl soyate of soybean oil and oleic acid will be part of the investigation. The structure of the final products will be characterized with GPC, IR, and NMR.

The objective of this research is to investigate the proposed reactions of cationic oligomerization of vegetable oils with superacids. Availability of the 4.6 double bonds/triglyceride in the soybean oil proves its potential ability to be oligomerized. It is known that soybean oil and fatty acid methyl esters of the soybean oil have the same double bonds in their structure and suggest that the oligomerization method of soybean oil can be used in the oligomerization of methyl esters

The potential applications of this investigation include new materials for the production of paints, inks, and as a part of the tire manufacture. Fatty acids are expected to produce lactones and estolides (Figure 3) such as lubricants, and dimer fatty acids have been used in synthesis of polyesters for polyurethane foams and coatings production.<sup>21</sup>

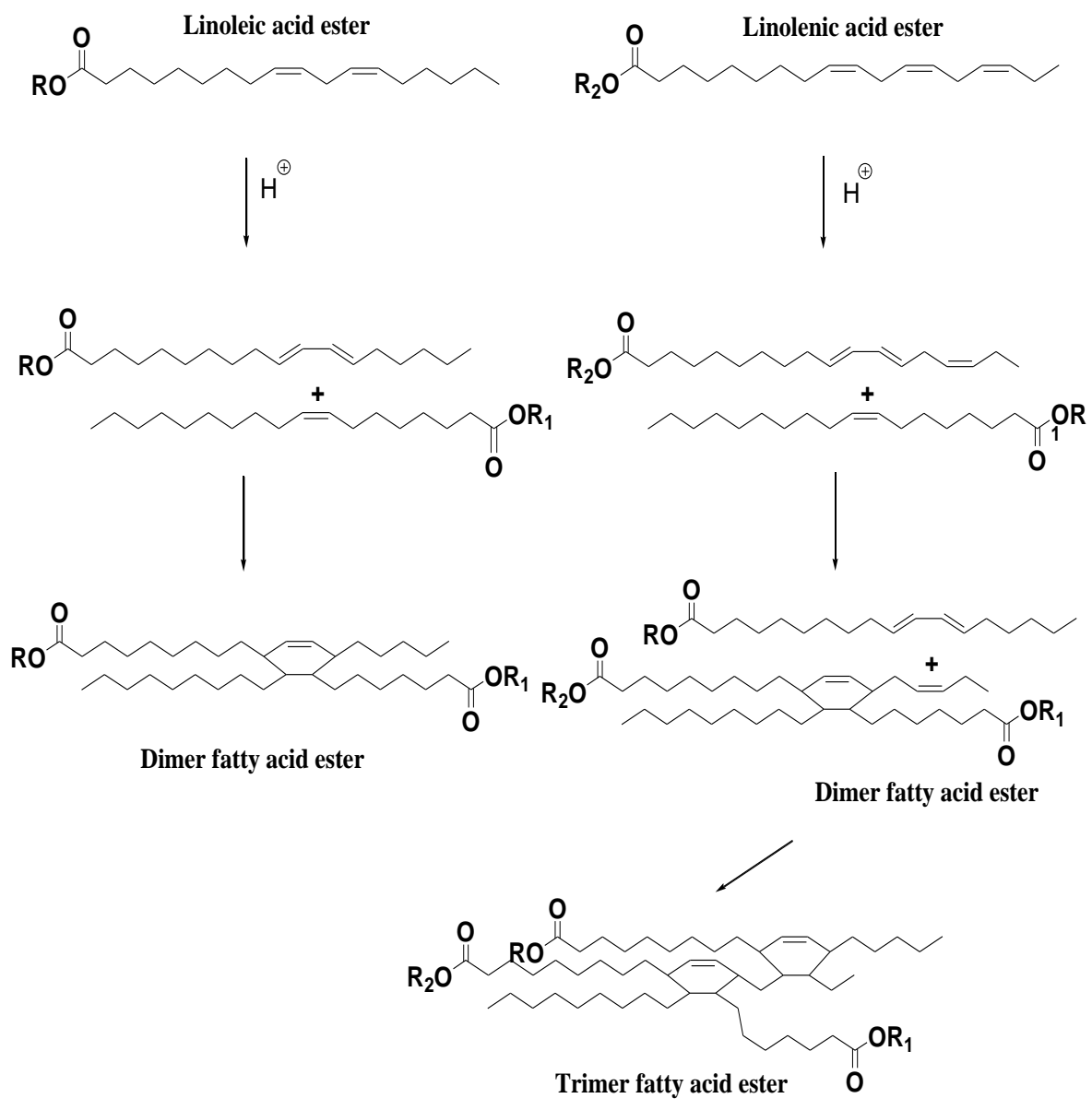
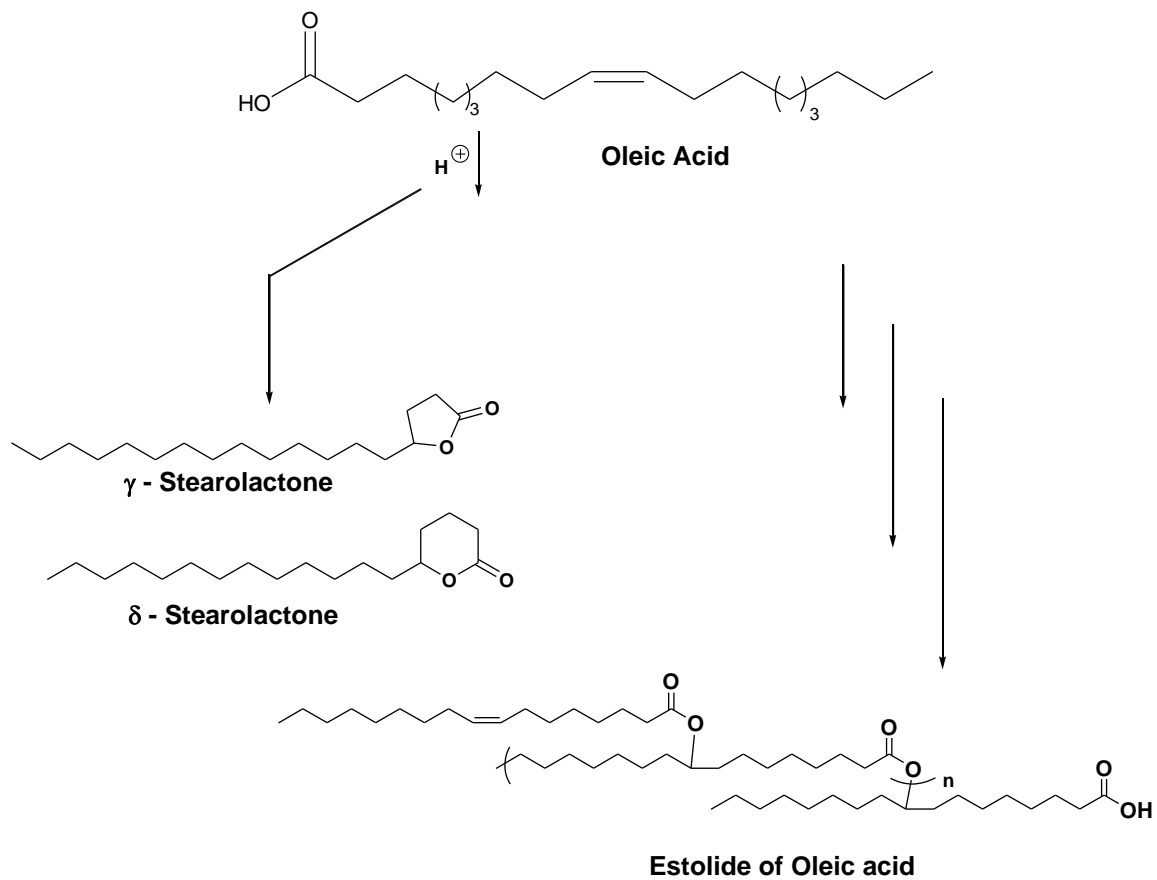


Figure 2. Proposed reaction of dimer and trimer fatty esters





**Figure 3. Formation of estolides and lactones from fatty acids**

## Chapter II

### 2. Experimental:

#### 2.1 Materials:

Samples of methyl esters (ME) were made by transesterification at KPRC. Oleic acid (OA) 90% pure was purchased from Alfa Aesar Chemical Company (Ward Hill, MA). Tetrafluoroboric acid diethyl ether complex was purchased from Sigma-Aldrich Chemical Company (St. Louis, MO) (catalyst) and used as received. Sodium bicarbonate for neutralization and hexane (HPLC grade) were commercially available and also used as received.

#### 2.2 Instrumentation:

Gel permeation chromatography (GPC) measurements were obtained using a JMDG-4 Waters 515 HPLC pump, a 2410 differential refractometer (Waters). Autosampler (SIL 20A, Shimadzu).  $M_n$  and  $M_w$  were calculated based on peaks present in chromatogram compared to polystyrene standard calibration. Fourier-transform Infrared Spectra (FT-IR) were using a Shimadzu IRAffinity-1. Nuclear magnetic resonance (NMR) spectra were using a Bruker DPX-300 spectrometer at a room temperature with deuterated chloroform ( $CDCl_3$ ) as a solvent in all experiments.

## **2.3 Methods:**

### **2.3.1 Transesterification:**

A round bottom flask equipped with magnetic stirrer was filled with 15 g of soybean oil and methanol. Potassium methoxide was added as a catalyst at 2 wt% of the oil. The mixture was refluxed for a three hours. The reaction was allowed to cool to room temperature and then a few drops of HCl were added to the mixture to neutralize the KOCH<sub>3</sub> with final pH value 6. The products were transferred to the separating funnel and extracted with 50 ml of hexane. Typically, the methyl esters phase was the upper layer and the glycerol phase was the lower layer. Glycerol was completely removed by washing two times with (75 ml) of distilled water and followed by two times with brine (50 ml) to remove residual methanol. The product was dried over sodium sulfate (Na<sub>2</sub>SO<sub>4</sub>) and the hexanes were removed under high vacuum. The final product was weighted and transferred to an airtight vial.

### **2.3.2 Oligomerization:**

A threaded vial was covered tightly with a rubber septum after drying by heated under vacuum to eliminate moisture. 5 g of the sample (methyl soyate or oleic acid) was added to each vial using a syringe. Tetrafluoroboric acid was added by syringe as a catalyst (Table 2, 3). The sample was transferred to an oven for 24 hours. The reaction mixture was allowed to cool to room temperature and then sodium bicarbonate was added to each sample to neutralize the HBF<sub>4</sub>. After adding (20 ml) of hexane, the resulting solution was followed by removal of the hexane under high vacuum. The final product was transferred to an airtight vial and weighed.

Two parameters were investigated in oligomerization. The first parameter was catalyst concentrations (1, 3, and 5 wt%) and the second parameter was temperature: 70, 90, 110, 130 °C.

**Table 2. Calculations of Monomer/Initiator ([M]/[I]) and double bond: Initiator ratios of Methyl Soyate samples**

Sample	Methyl Soyate		mmol of	Catalyst		[M] / [I]	(D.B/I)
	(g)	(mmol)	D.B	(wt)%	(mmol)		
MS-1	5	17	24	1	0.57	29.92	42.24
MS-3	5	17	24	3	1.71	9.94	14.04
MS-5	5	17	24	5	2.84	5.99	8.45

Double bond

(Monomer: initiator) ratio

(Double bond: initiator) ratio

**Table 3. Calculations of Monomer/Catalyst ([M]/[I]) and double bond: Catalyst ratios of Oleic acid samples**

Sample	Oleic acid		mmol of	Catalyst		[M] / [I]	D.B/I
	(g)	(mmol)	D.B	(wt)%	(mmol)		
OA-1	5	18	18	1	0.57	31.68	31.68
OA-3	5	18	18	3	1.71	10.53	10.53
OA-5	5	18	18	5	2.84	6.34	6.34

## Chapter III

### 3. Results and discussion:

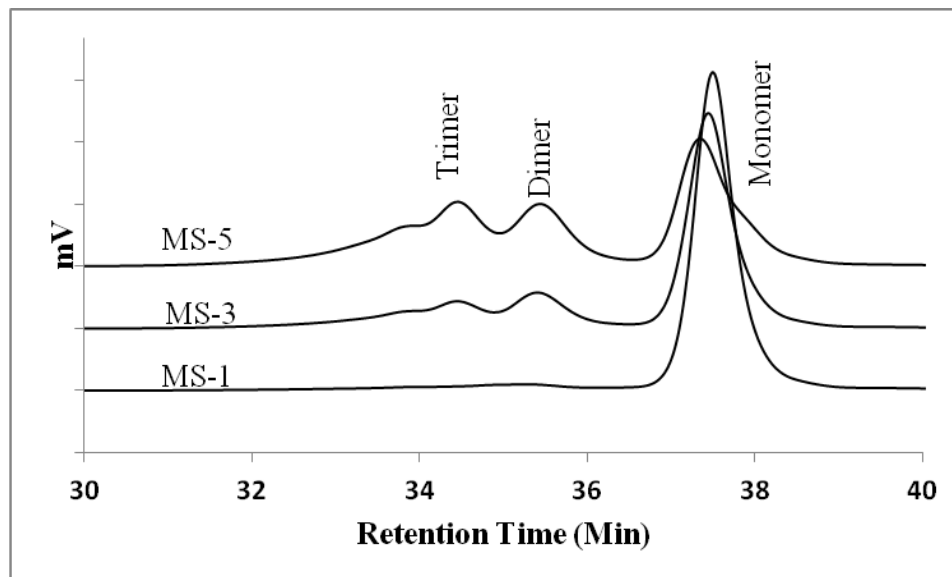
#### 3.1 The Effect of Catalyst Concentration:

Table 4 shows the yields of materials obtained from methyl soyate and oleic acid samples with different concentrations of tetrafluoroboric acid  $\text{HBF}_4$  as an initiator at 90 °C.

**Table 4. Calculation of the yield of Methyl soyate and Oleic acid after filtration**

Sample	Yield		
	Theoretical (g)	Actual (g)	%
MS-1	5	4.8	96
MS-3	5	4.7	94
MS-5	5	4.6	93
OA-1	5	4.3	86
OA-3	5	4.2	84
OA-5	5	4.3	86

### 3.1.1 Gel Permeation Chromatography (GPC):



**Figure 4. GPC trace of MS oligomerized samples**

Figure 4 shows methyl soyate samples have three different fractions. Peak one in MS-1 (monomer) has an area of 94.9% unreacted methyl soyate, while peak two in MS-1 (dimer) has an area of 5.08% (Table 5). The weight average molecular weights increased from MS-1 (261.4 g/mol) to MS-5 (597.45g/mol) suggesting an increase in the oligomerization. The polymeric product contained 43-95% monomer, 5-22% dimer, and 17-36% trimer. As a result, increasing the amount of the catalyst increased the formation of dimer and trimer of MS-3 and MS-5, while, the percentage of the monomer decreased from MS-1 94.9% to 42.59% in MS-5 due to the oligomerization of the methyl soyate.

**Table 5. Mw of MS oligomerized samples from GPC**

Sample	Peak 1		Peak 2		Peak 3		Mw
	Mp	%Area	Mp	%Area	Mp	%Area	
MS-1	238	95	583	5	0	0	261
MS-3	243	70	553	14	814	17	421
MS-5	253	43	546	22	813	36	598

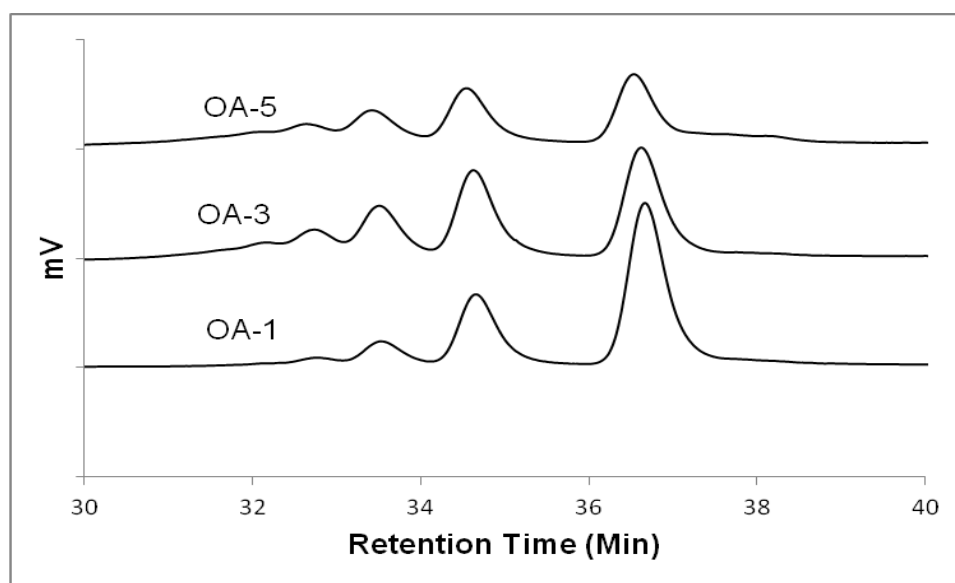
**Figure 5. GPC trace of OA oligomerized samples**

Figure 5 shows oleic acid samples have five peaks. Peak one in OA-1, OA-3, and OA-5 are the monomer. Peak one in OA-1 has a %area of 61% and peak three has an area 26.6%, while peak four has an area of 4% (Table 6). The weight average molecular weight increased from 484 for OA-1 to 820 in OA-5. The polymeric product contained 37-61% monomer, 27-29% dimer, 9-18% trimer, 4-10% tetramer, and 7-8% pentamer. As a result, increasing the concentration of the catalyst showed increasing amounts of dimer and other oligomers.

**Table 6. Mw of OA oligomerized samples from GPC**

Sample	Peak 1		Peak 2		Peak 3		Peak 4		Peak 5		Mw
	Mp	%Area	Mp	%Area	Mp	%Area	Mp	%Area	Mp	%Area	
OA-1	284	61	647	26.6	1026	9	1409	4	0	0	484
OA-3	289	37	655	28.94	1036	18	1419	9	1793	7.7	813
OA-5	300	38	677	26.74	1074	17	1478		1849	7.9	820

### 3.1.2 Fourier Transform Infrared Spectroscopy (FTIR):

Figure 6 shows FTIR of MS samples. The FTIR spectra showed a carbonyl stretch corresponding to an ester group at  $1743\text{ cm}^{-1}$ . In addition, the peak at  $1458\text{ cm}^{-1}$  indicates a C=C stretch vibration. Absorption peak at around  $3010\text{ cm}^{-1}$  indicates an unsaturation C-H. Moreover, multiple peaks at  $1050\text{--}1360\text{ cm}^{-1}$  correspond to a C-O. Also, strong peak at around  $2854\text{ cm}^{-1}$  and  $2924\text{ cm}^{-1}$  indicating a stretch from a saturated C-H.

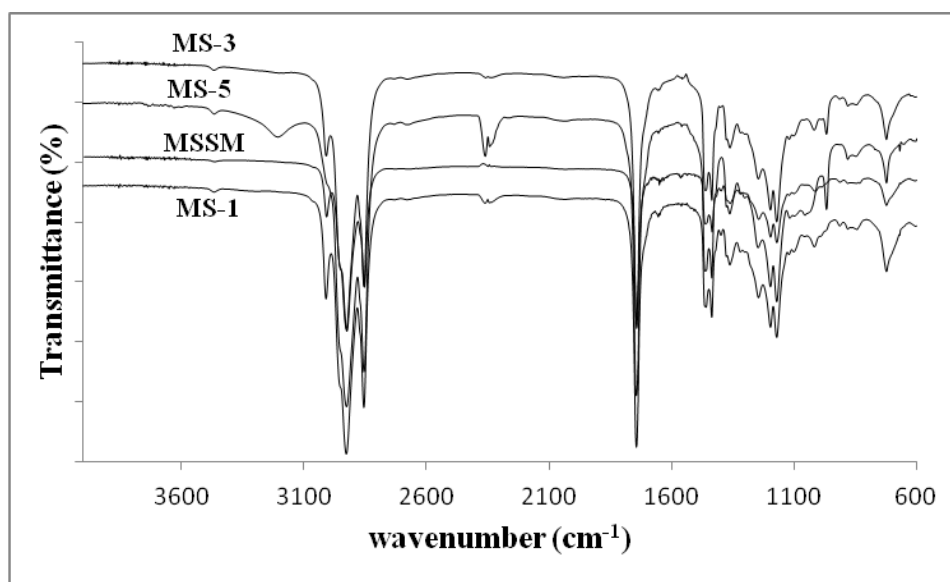
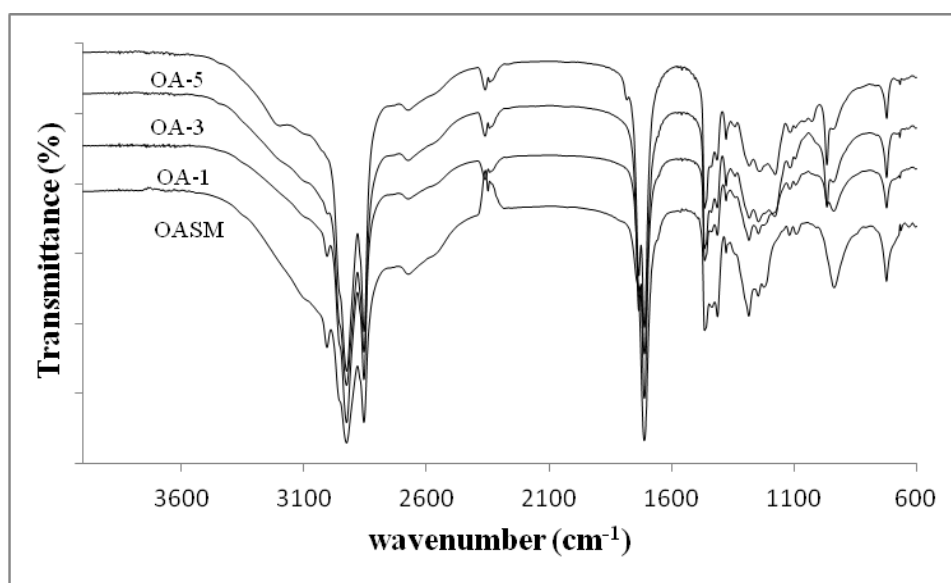
**Figure 6. FTIR spectra of MS-1, MS-3, and MS-5 samples**

Figure 7 shows FTIR spectra of OA-1, OA-3, and OA-5 samples. The FTIR spectra showed two carbonyl groups, one at  $1712\text{ cm}^{-1}$  corresponding to a carboxylic acid and the other carbonyl group at a  $1735\text{ cm}^{-1}$  corresponds to an ester. Moreover, the peak



at  $1467\text{ cm}^{-1}$  medium peak was consistent with a C=C stretch. In addition, multiple peaks from  $1120\text{ cm}^{-1}$  to  $1356\text{ cm}^{-1}$  are stretching from a C-O. In addition, broad peak from  $3000\text{ cm}^{-1}$  to around  $3400\text{ cm}^{-1}$ , indicates an OH group stretching from carboxylic acid which decreased with increasing catalyst concentration. Also, a strong peak at  $2854\text{ cm}^{-1}$  and  $2924\text{ cm}^{-1}$  corresponds to stretching from C-H. Finally, a peak at around  $3010\text{ cm}^{-1}$  from =C-H stretching decreased with increasing catalyst concentration due to the formation of estolides and lactones.



**Figure 7. FTIR spectra of OA-1, OA-3, and OA-5 samples**

### **3.1.3 Nuclear Magnetic Resonance (NMR):**

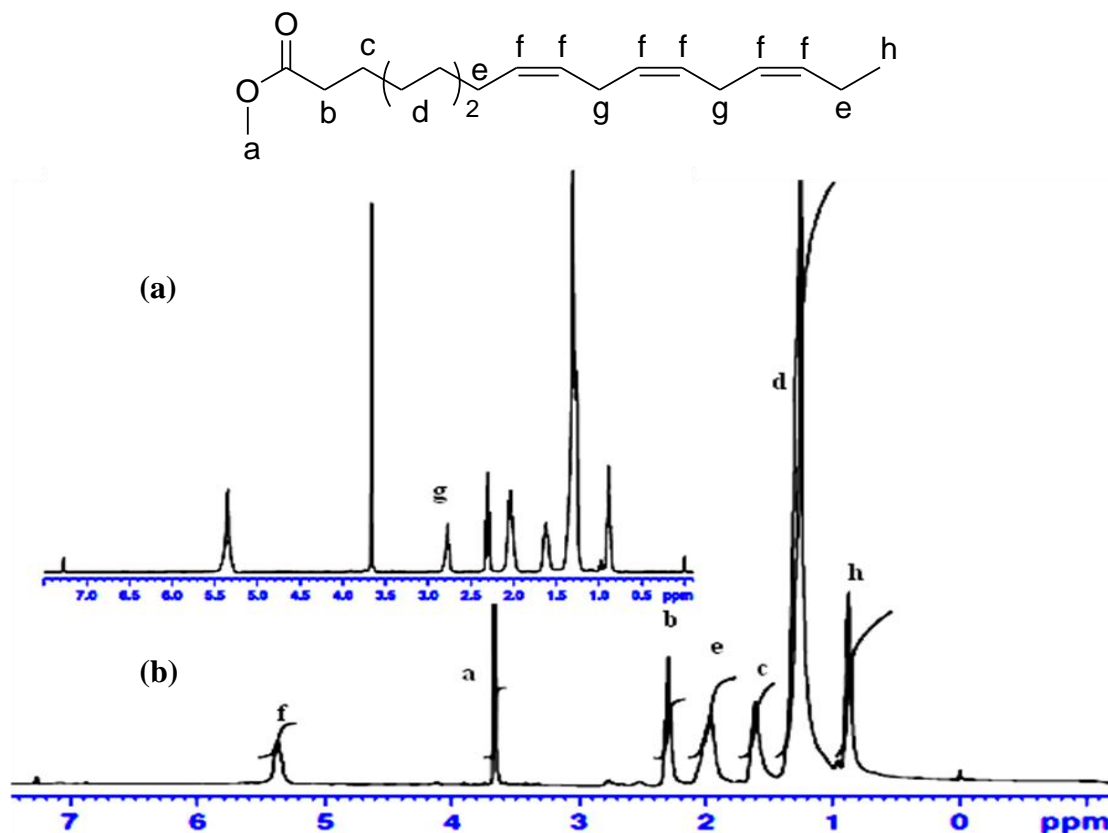
Figure 8 (a) and (b) show the  $^1\text{H}$  NMR spectra of methyl soyate starting material and MS-5 sample. Comparing to literature, the  $^1\text{H}$  NMR chemical shifts of methyl soyate were assigned.<sup>22</sup> Methyl soyate starting material and MS-5 have two methyl groups. The first methyl group at 0.9 ppm was the terminal methyl group peak connected to  $\text{CH}_2$  and the other methyl group at 3.6 ppm was connected to the ester oxygen. The next peak between 1.2-1.5 ppm corresponds to the  $(\text{CH}_2)_4$  and peak at around 1.6-1.7 ppm indicates

to (CH<sub>2</sub>) β to carbonyl group. In addition, the peak at 2 ppm indicated allylic protons. Moreover, peak at around 2.3 ppm corresponds to CH<sub>2</sub> α to carbonyl group. Also, the peak at 2.8 ppm indicates the bis-allylic protons in MSSM which disappeared in MS-5 due to the migration of double bonds. Moreover, the peak at around 5.4 ppm the methyl soyate structure corresponds to olefinic protons. The reference ratio between the area under the peak of methyl group with letter (h) in the structure and the area under the peak of double bond with letter (f) (CH=CH) is 3:2. Calculation the double bonds reduction of all MS samples provided the number of double bonds that consumed during the reaction. Also, a peak after 5.4 ppm would have indicated cyclization of the MS-5 oligomerized sample. However, there was any peak after 5.4 ppm.

Table 7 shows the number of double bond that decreased from 1.58 in methyl soyate starting material to 0.36 in MS-5. While, the double bonds reduction and the iodine value reduction increased respectively, due to the oligomerization of the double bonds in methyl soyate.

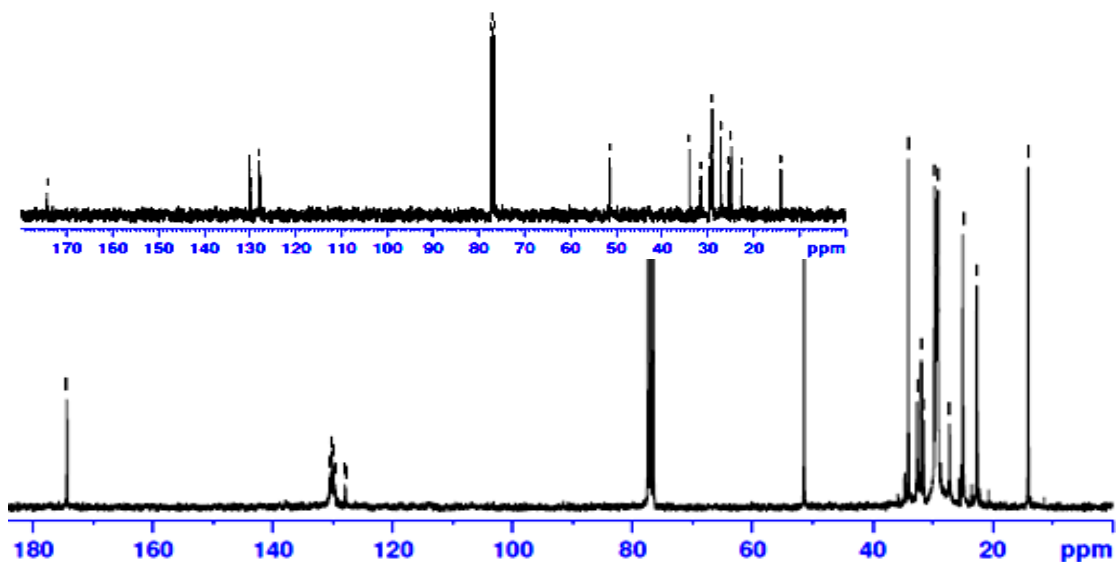
**Table 7. Double bonds reduction of MS samples**

Sample	Area of CH <sub>3</sub> group	Area of CH	Double bond	D.B reduction %	I.V reduction %	Acid Value
MSSM*	0.95	1	1.58	0	0	2
MS-1	1.22	1	1.23	22	11	10
MS-3	1.89	1	0.8	49	12	25
MS-5	4.23	1	0.36	77	21	30



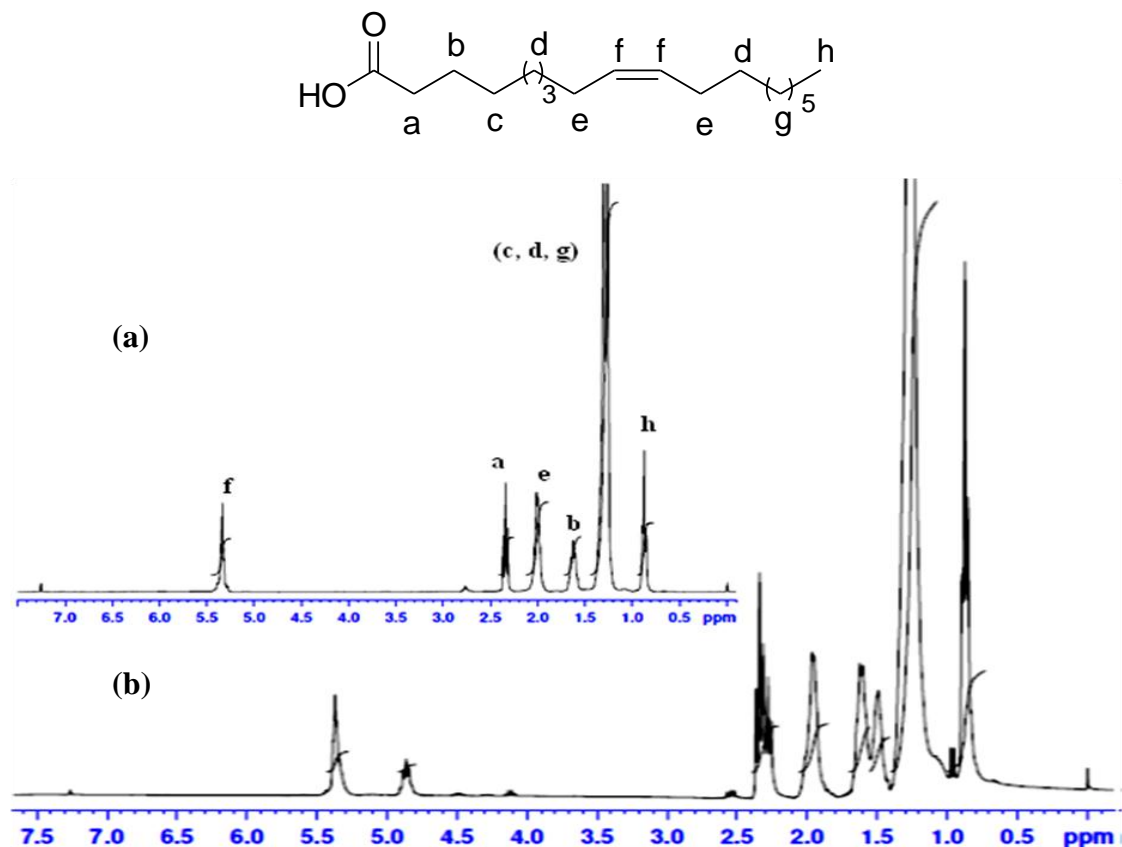
**Figure 8.** <sup>1</sup>H NMR spectra (a) MS starting material, (b) MS-5 oligomerized sample

Figure 9 shows the <sup>13</sup>C NMR spectra of MS starting material and MS-5 sample. The <sup>13</sup>C NMR spectra of MS starting material and MS-5 are identical except for the changes in peak intensities. Two carbons from methyl groups appeared in the C structure. The first carbon from the methyl group connected to a CH<sub>2</sub> appears at 14.3 ppm. The second carbon from the methyl group connected to an ester group appeared at 51.6 ppm. Next, peaks at around 22.5-34.6 ppm indicated (CH<sub>2</sub>)<sub>10</sub> protons. The MS-5 has more carbon peaks in this range due to the reducing the double bonds of methyl soyate. Moreover, peaks at 127.8-130 ppm corresponded to of the double bond carbons. Finally, the peak at 174.2 ppm indicated a carbonyl group. Also, peaks around 40 ppm would have indicated a methine carbon due to a cyclization reaction in the MS-5 oligomerized sample but no peaks at 40 ppm were observed.



**Figure 9.**  $^{13}\text{C}$  NMR spectra (a) MS starting material (b) MS-5 oligomerized sample

Figure 10 shows the  $^1\text{H}$  NMR spectra of Oleic acid starting material and OA-5 oligomerized sample. The peak at 2.2 ppm indicates a  $\text{CH}_2$   $\alpha$  to an ester carbonyl. The peak at 2.3 ppm is the  $\text{CH}_2$   $\alpha$  to carboxylic acid group.<sup>15</sup> Moreover, the peak at 2.5 ppm corresponds to a  $\gamma$ -stearolactone. Also, the peak at 4.2 ppm indicated to  $\delta$ -stearolactone. In addition, the peak at 4.5 ppm corresponded to  $\gamma$ -stearolactone.<sup>23</sup> Finally, a peak at 4.8 ppm CH indicates to the linkage of estolides structure.<sup>24</sup>



**Figure 10. <sup>1</sup>H NMR spectrum of (a) OA starting material (b) OA-5 oligomerized sample**

Table 8 shows the number of double bonds of oleic acid starting material decreased from 1.04 to 0.3 in OA-5 sample. The double bond reduction increased from 52% in OA-1 oligomerized sample to 71% in OA-5 oligomerized sample. In addition, the iodine value increased with increasing the catalyst concentration. Also, the acid value decreased from 202 mg KOH/g in OASM to 133 mg KOH/g in OA-5 oligomerized sample due to the formation of estolides and lactones.

**Table 8. Double bonds reduction of Oleic acid samples**

Sample	Area of CH <sub>3</sub> group	Area of CH	Double bond	D.B reduction %	I.V reduction %	Acid Value
OASM*	1.44	1	1.04	0	0	202
OA-1	3.02	1	0.5	52	29	145
OA-3	3.24	1	0.47	55	39	127
OA-5	5.03	1	0.3	71	49	133

\*Oleic acid starting material

Figure 11 shows  $^{13}\text{C}$  NMR spectra of oleic acid starting material and OA-5 oligomerized sample. Peak at 14 ppm with letter (e) of the oleic acid structure indicates a methyl group. Peaks from 22 ppm to 36 ppm corresponded to  $\text{CH}_2$  of the fatty acid chain. Moreover, peak at 130 ppm indicates a double bond carbon. Also, the peak at 127 ppm with letter (c) corresponds to an impurity. In addition, the distinguishable peak at 73 ppm was consistent with a methine carbon from an estolides.<sup>15</sup> Finally, two different peaks from carbonyls were observed. The first peak at 173.8 ppm was from an ester estolides and the other peak at 180 ppm was from the carboxylic acid.<sup>24</sup>

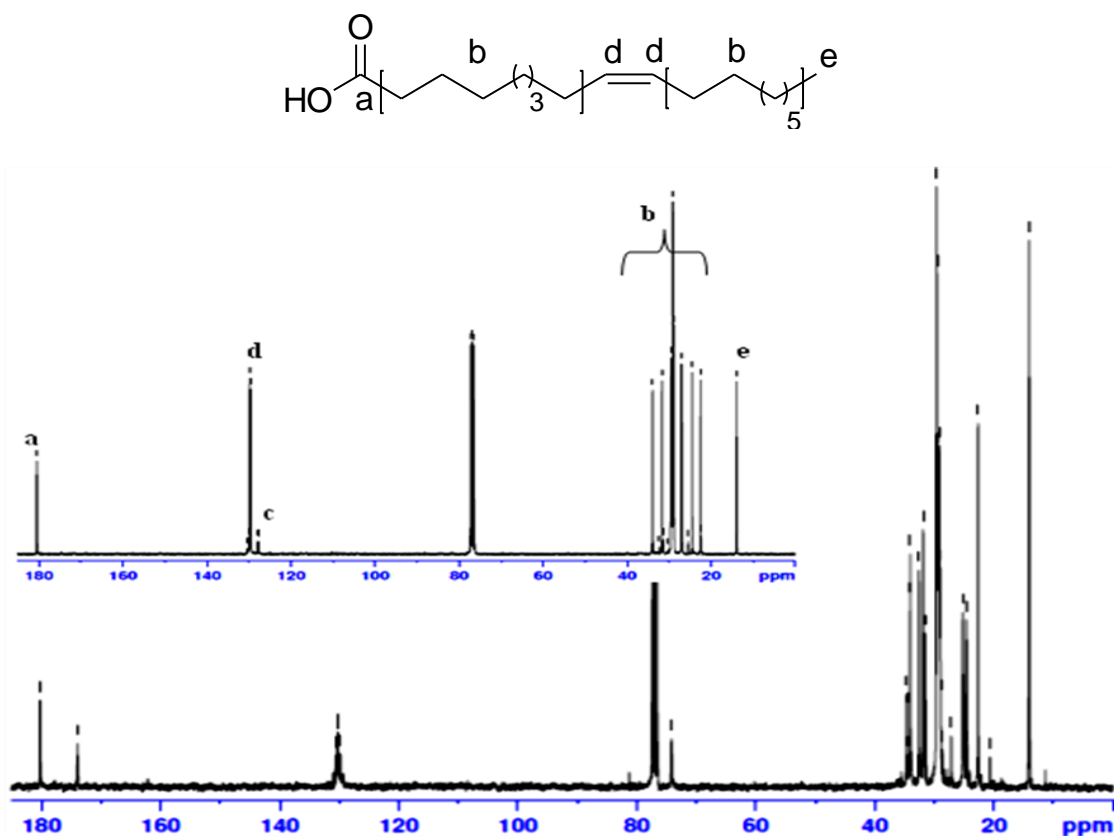


Figure 11.  $^{13}\text{C}$  NMR spectrum of (a) OA starting material (b) OA-5 oligomerized sample

### 3.2 The Effect of Temperature:

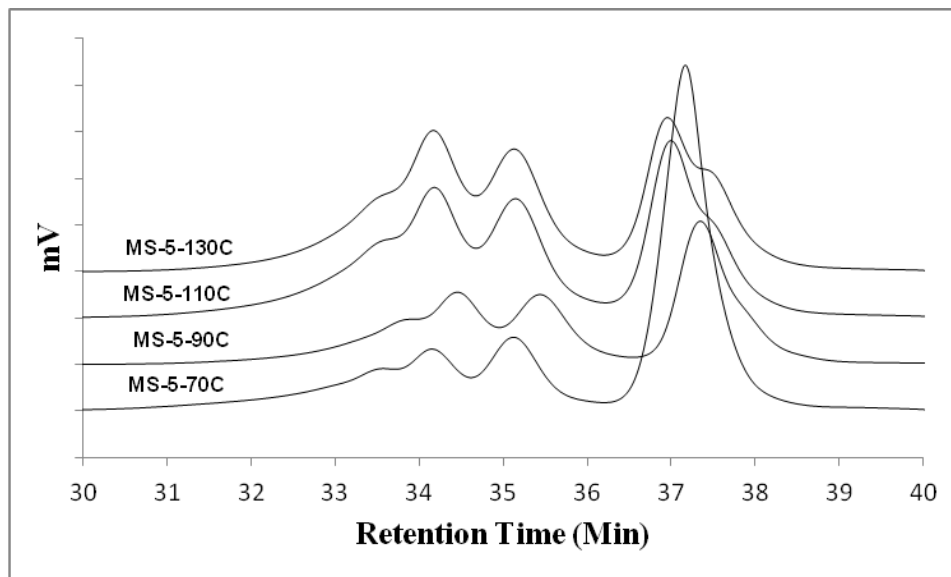
Table 9 shows the yields of methyl soyate and oleic acid with the same concentrations of tetrafluoroboric acid at different temperatures: 70, 90, 110, and 130 °C.

**Table 9. Calculation the yield of Methyl soyate and Oleic acid after filtration**

Sample	Yield		
	Theoretical (g)	Actual (g)	%
MS-5-70C	5	4.6	92
MS-5-90C	5	4.6	93
MS-5-110C	5	4.1	82
MS-5-130C	5	4.7	94
OA-5-70C	5	4.8	96
OA-5-90C	5	4.3	86
OA-5-110C	5	4.5	90
OA-5-130C	5	4.6	92



### 3.2.1 Gel Permeation Chromatography (GPC):



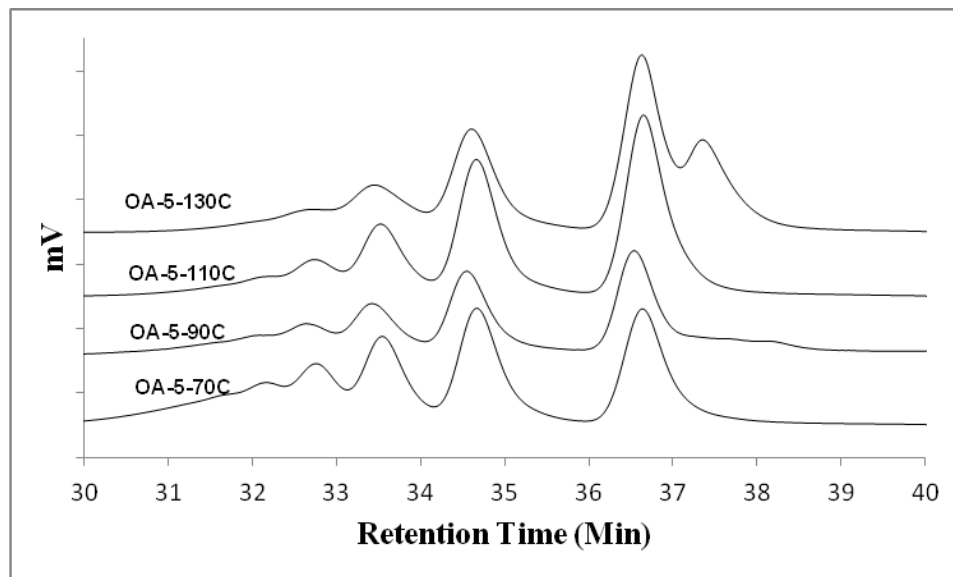
**Figure 12. GPC trace of MS-5 oligomerized samples at different temperature**

Figure 12 shows GPC results of the methyl soyate samples oligomerized at different temperatures. Peak one in MS-5-70C, MS-5-110C, and MS-5-130C oligomerized samples were the monomer. Peak one in MS-5-70C (monomer) has a percent area of 61.5% of initial MS-5-70C sample remains unreacted while peak two in the same sample (dimer) had the lowest area number 14.6% (Table 10). This results showed that the percent area of the monomer decreased, while, the dimer and other oligomers increased with increasing the temperatures. Moreover, a small shoulder appeared at lower molecular weight that the monomer of the MS-5-130C suggesting indicating the formation of a new compound at a lower molecular weight than the starting material. The weight average molecular weights increased from MS-5-70C (494.9 g/mol) to MS-5-110C (622g/mol) except MS-5-130C (603.9 g/mol) due to the chain scission. The polymeric product contained 36.1-61.5% monomer, and the remaining were oligomers: 14.6-24.4% dimer and 23.9- 40.5% trimer. The percent area

of oligomers increased from 38.5 % in MS-5-70C oligomerized sample to 63% in MS-5-110C oligomerized sample that was consistent with cationic oligomerization.<sup>15</sup>

**Table 10. Mw of MS oligomerized samples from GPC**

Sample	Peak 1		Peak 2		Peak 3		Mw
	Mp	% Area	Mp	% Area	Mp	% Area	
MS-5-70C	232	62	535	15	796	24	495
MS-5-90C	253	43	546	22	813	36	598
MS-5-110C	249	37	530	23	787	41	622
MS-5-130C	253	36	534	24	791	40	604



**Figure 13. GPC trace of OA oligomerized samples at different temperature**

Figure 13 shows that the Oleic acid oligomerized samples have five fractions. The monomer fraction increased while the other oligomers fractions decreased with increasing the temperatures. The weight average molecular weight decreased from OA-5-70C oligomerized sample with 1035.6 g/mol to 564.7 g/mol in OA-5-130C oligomerized (Table 11). The monomer of the OA-5-130C has a small shoulder due to low molecular

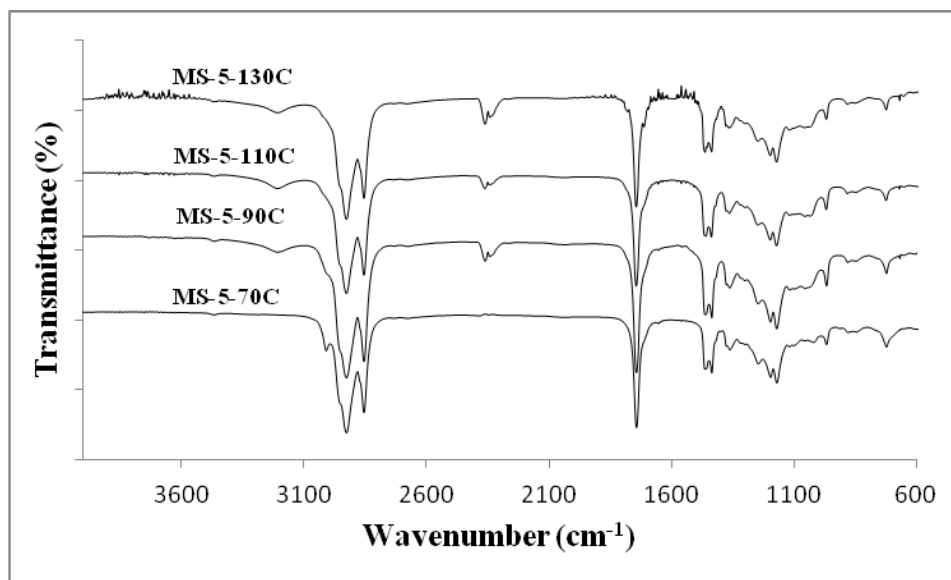
weight compound from chain scission. The molecular weight decreased in the OA-5-130C due to the low weight material formed during the oligomerization.

**Table 11. Mw of OA oligomerized samples from GPC**

Sample	Peak 1		Peak 2		Peak 3		Peak 4		Peak 5		Mw
	Mp	%Area	Mp	%Area	Mp	%Area	Mp	%Area	Mp	%Area	
OA-5-70C	288	26	645	25	1022	19	1409	12	1795	18	1036
OA-5-90C	300	38	677	27	1074	17	1478	10	1849	8	820
OA-5-110C	286	40	646	30	1030	17	1419	13	0	0	705
OA-5-130C	289	55	661	25	1061	20	0	0	0	0	565

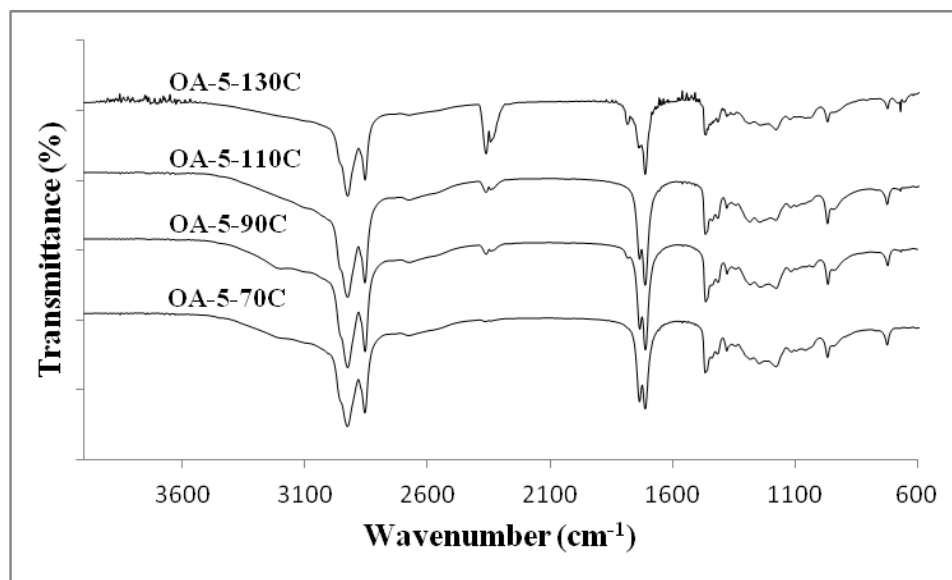
### 3.2.2 Fourier Transform Infrared Spectroscopy (FTIR):

Figure 14 shows the FTIR spectra of MS-5 oligomerized samples at different temperatures. From analyzing FTIR spectra, there was a carbonyl stretch corresponding to ester at  $1743\text{ cm}^{-1}$ . In addition, a peak at  $1458\text{ cm}^{-1}$  indicated a C=C stretch. Also, strong peak at around  $2854\text{ cm}^{-1}$  and  $2924\text{ cm}^{-1}$  indicated stretching from C-H. Moreover, a medium peak at  $3010\text{ cm}^{-1}$  for in MS-5-70C was due to stretching from =C-H appeared. Also, small shoulder peaks at around  $3200\text{ cm}^{-1}$  may indicate an OH group not presents in the starting sample for MS-5-70C. This peak started to appear in the MS-5-90C, MS-5-110C, and MS-5-130C and may be due to the formation of a low weight molecular weight compound from chain scission.



**Figure 14. FTIR spectrum of MS-5 oligomerized samples at different temperatures**

Figure 15 shows the FTIR spectra of OA-5 oligomerized samples at different temperatures. From analyzing the FTIR spectra there are two carbonyl groups in OA-5-70C, OA-5-90C, and OA-5-110C. The first peak at  $1712\text{ cm}^{-1}$  corresponds to a carboxylic acid and the other carbonyl group at  $1735\text{ cm}^{-1}$  corresponds to an ester. OA-5-130C had multiple carbonyls suggesting the formation of additional carbonyls besides estolides and lactones. Moreover, the medium peak at  $1467\text{ cm}^{-1}$  indicated a C=C stretch. In addition, multi medium peaks from around  $1120\text{ cm}^{-1}$  to  $1356\text{ cm}^{-1}$  was consistent with a C-O. In addition, broad peak from  $3000\text{ cm}^{-1}$  to around  $3400\text{ cm}^{-1}$  indicates OH stretching from a carboxylic acid which decreased in intensity with increased the temperatures. Also, a strong peak at around  $2854\text{ cm}^{-1}$  and  $2924\text{ cm}^{-1}$  indicated stretching from a C-H.



**Figure 15. FTIR spectrum of OA-5 oligomerized samples at different temperatures**

### 3.2.3 Nuclear Magnetic Resonance (NMR):

Figure 16 (a) and (b) show  $^1\text{H}$  NMR spectra of methyl soyate starting material and MS-5-90C. They have two methyl groups. The first terminal methyl group appeared as a triplet at 0.9 ppm and the methyl attached to the ester oxygen as a singlet at 3.6 ppm. The peak is between 1.2-1.5 ppm corresponded to the  $(\text{CH}_2)_4$  groups and the peak at 1.6-1.7 ppm was consistent with a  $(\text{CH}_2)$   $\beta$  to the carbonyl group. In addition, the peak at 2 ppm indicated the allylic group connected to  $\text{CH}_3$ . Moreover, the peak at 2.3 ppm corresponded to the  $\text{CH}_2$   $\alpha$  to carbonyl group. Also, the peak at 2.8 ppm indicated bis-allylic protons which appeared in MSSM but disappeared in MS-5-90C due to the migration of double bonds. There were no changes in the spectrum for MS-5-70C  $^1\text{H}$  NMR. However, the changes observed for MS-5-90C, also, occurred for MS-5-110C and MS-5-130C. The reference ratio between the area of methyl group and the area of CH double bond ( $\text{CH}=\text{CH}$ ) is 3:2 (Table 12).

The number of double bond decreased from 0.75 in MS-5-70C to 0.23 in MS-5-130C due to consumption of double bond, whereas, the double bond reduction is increasing from 53% in MS-5-70C oligomerized sample to 85% in MS-5-130C oligomerized sample due to the oligomerization of the double bonds in MS samples (Table 12). The iodine value increased slightly with increasing temperature which was consistent with the NMR showing a decrease in the number of double bonds.

**Table 12. Double bonds reduction of MS samples in different temperatures**

Sample	Area of CH <sub>3</sub> group	Area of CH	Double bond	Double bond reduction %	I.V reduction %
MS-5-70C	2.03	1	0.75	53	16
MS-5-90C	4.23	1	0.36	77	21
MS-5-110C	6.08	1	0.25	84	20
MS-5-130C	4.23	1	0.23	85	23

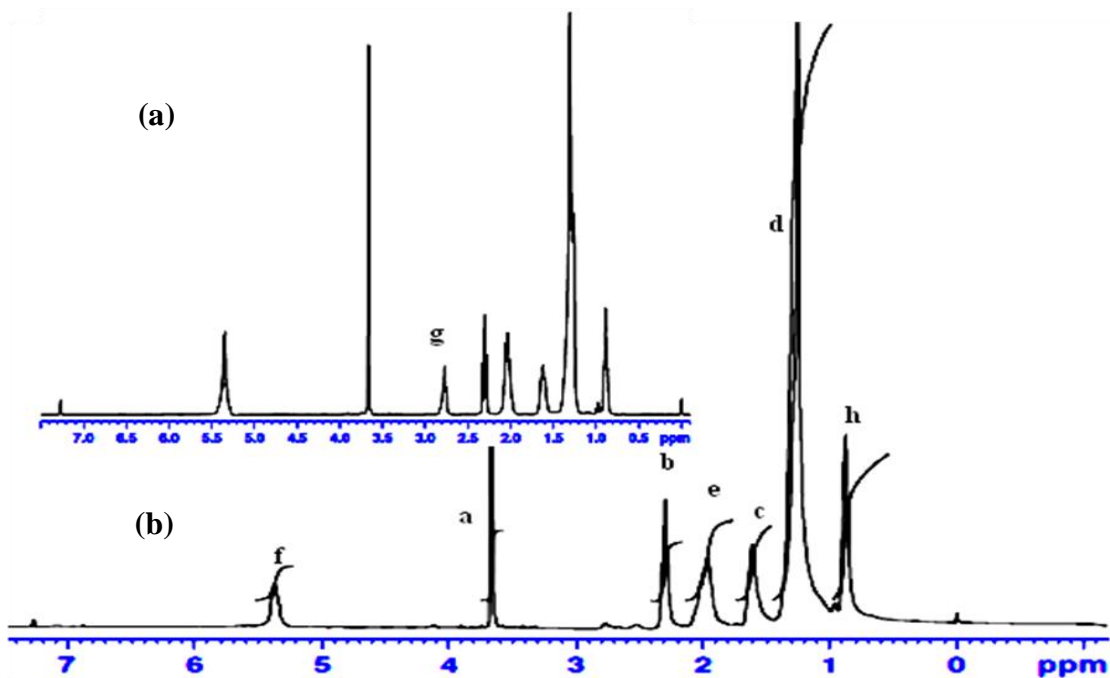
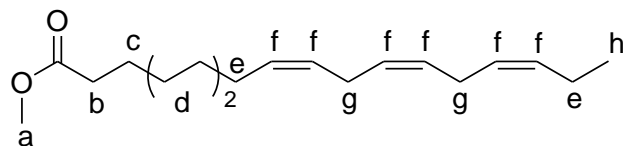
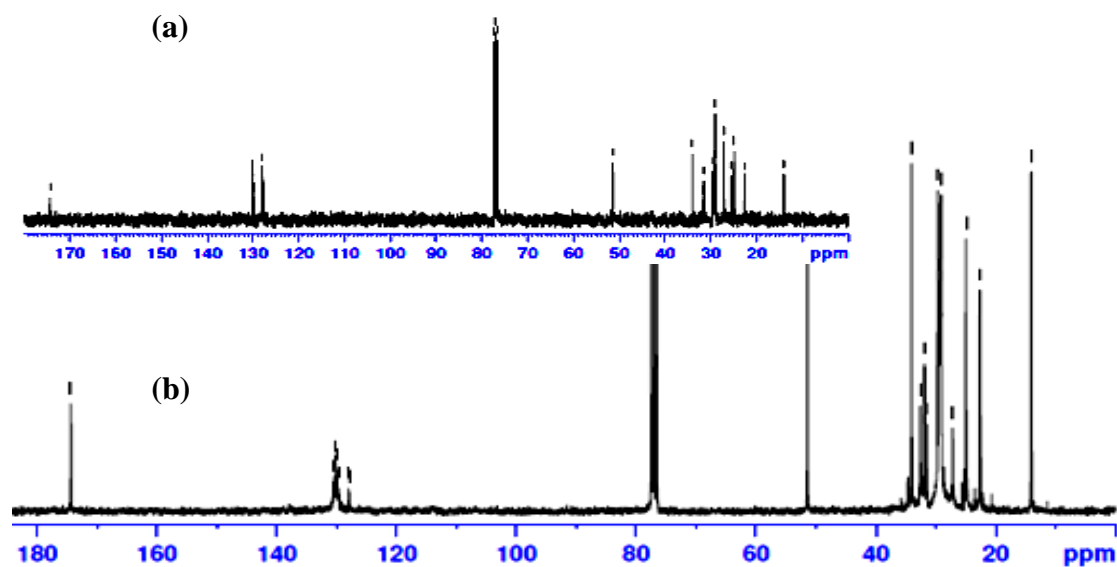


Figure 16.  $^1\text{H}$  NMR spectra (a) MS starting material, (b) MS-5-90C oligomerized sample

Figure 17 shows the  $^{13}\text{C}$  NMR spectra of MS starting material and MS-5-90C oligomerized sample. The two spectra are similar except for the intensities of the peaks. The  $^{13}\text{C}$  NMR spectra of MS starting material and MS-5-90C have two carbons from methyl groups. The first carbon was from the methyl group connected to a carbon( $\text{CH}_2$ ) at 14.3 ppm. The second carbon was from the methyl group connect to the ester group and appeared at 51.6 ppm. Moreover, peaks around 127.8-130.1 ppm indicated the double bond carbons. Finally, a peak around 174.2 ppm corresponded to a carbonyl group from an ester. The  $^{13}\text{C}$  NMR spectra of MS-5-70C, MS-5-110C and MS-5-130C oligomerized samples were similar to MS-5-90C.

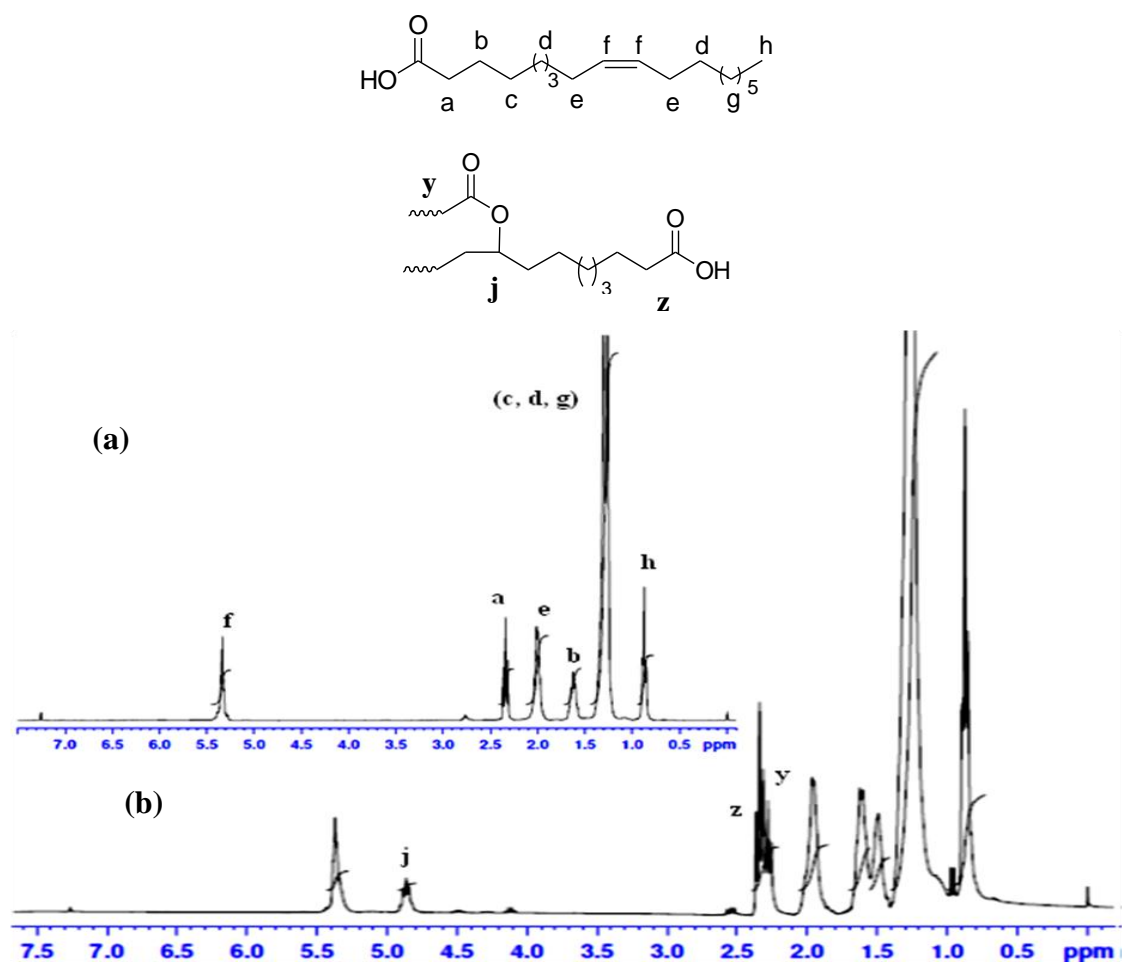


**Figure 17.  $^{13}\text{C}$  NMR spectra (a) MS starting material (b) MS-5-90C oligomerized sample**

Figure 18 shows the  $^1\text{H}$  NMR spectra of Oleic acid starting material (OASM) and OA-5-90C oligomerized sample. A peak at around 2.3 ppm in OASM indicated methylene protons  $\alpha$  to a carbonyl group from a carboxylic acid and the peak at 2.2 ppm indicated a



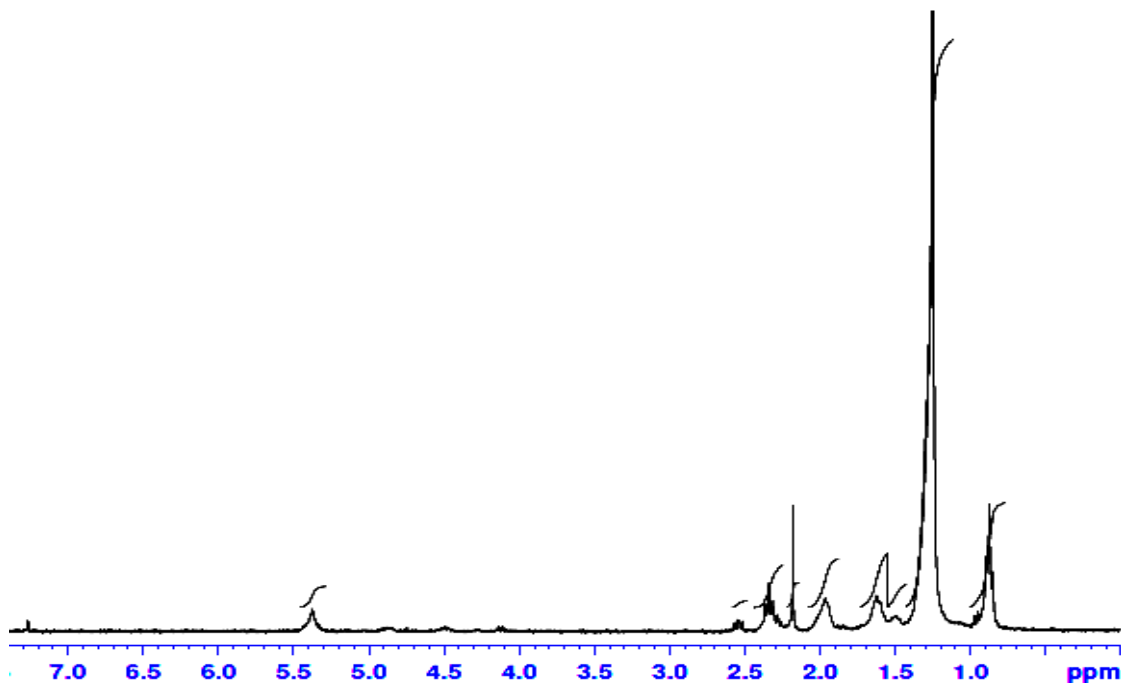
CH<sub>2</sub> α to an ester group.<sup>24</sup> In addition; the peak in OA-5-90C at 4.8 ppm was from the CH of the estolides structure.<sup>25</sup> Moreover, there are three small peaks appearing in OA-5-90C and OA-5-130C oligomerized samples. The first peak at 2.5 ppm indicated a CH<sub>2</sub> α to the carbonyl group from a γ-stearolactone. The second peak at 4.2 ppm corresponded to a CH from a δ-stearolactone. The third peak at 4.5 ppm indicated aCH from a γ-stearolactone.<sup>23</sup> Finally, at 5.3 ppm appeared a peak corresponding to olefinic protons in OASM and MS-5-90C.



**Figure 18.** <sup>1</sup>H NMR spectra of (a) OA starting material (b) OA-5-90C oligomerized sample

Figure 19 showed similar peaks compared to the <sup>1</sup>H NMR spectrum of OA-5-90C except for the intensities of the peaks. In addition, a very small peak at 4.8 ppm indicated

estolide linkages which decreased with increasing temperature. Also, the peaks at 2.5 ppm, 4.2 ppm, and 4.5 ppm indicated  $\delta$ -stearolactone and  $\gamma$ -stearolactone formation which decreased with increasing temperatures.



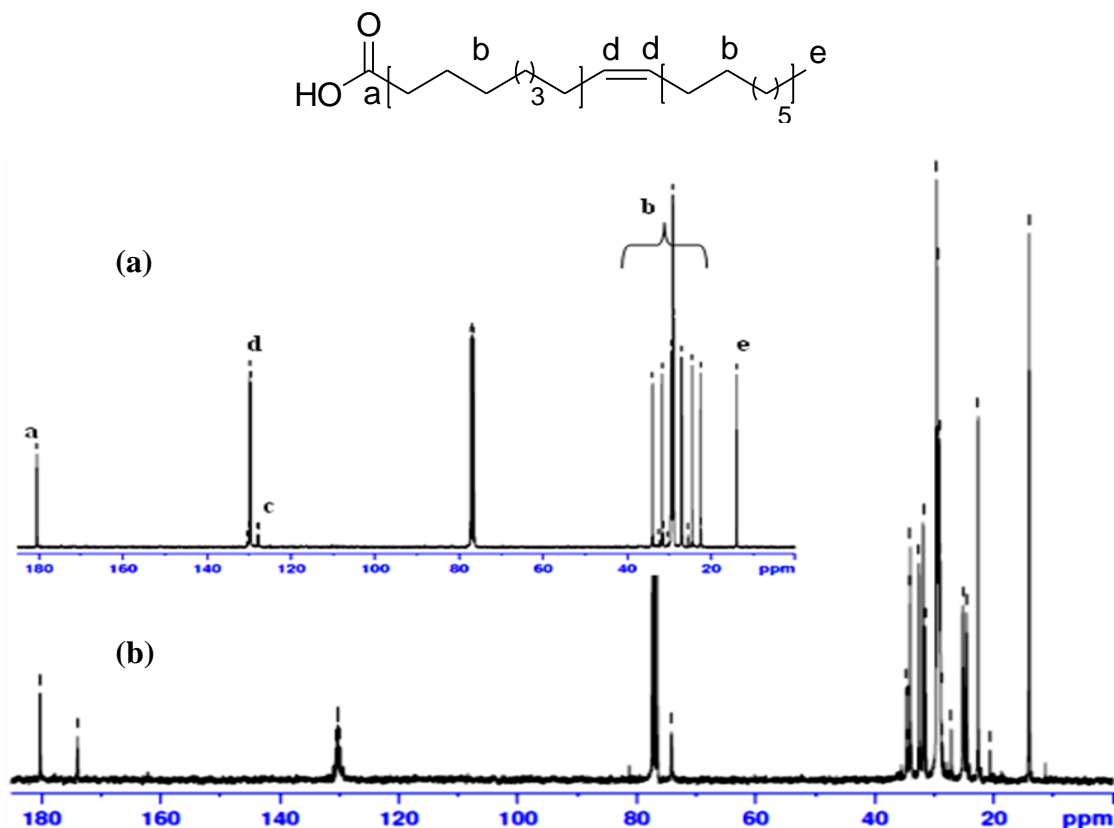
**Figure 19.**  $^1\text{H}$  NMR spectrum OA-5-130C oligomerized sample

Table 13 shows that the number of double bonds decreased in OA-5-70C to OA-5-130C due to the formation of estolides, lactones, and a new low weight molecular weight compound. The double bond reduction increased in the OA-5-70C oligomerized sample compared to the OA-5-130C oligomerized sample. The iodine value reduction decreased with increases the temperatures.

**Table 13. Double bonds reduction of Oleic acid samples**

Sample	Area of CH <sub>3</sub> group	Area of CH	Double bond	Double bond reduction %	I.V reduction %
OA-5-70C	4.77	1	0.32	69	46
OA-5-90C	5.03	1	0.3	71	49
OA-5-110C	4.00	1	0.38	64	41
OA-5-130C	5.03	1	0.3	71	33

Figure 20 shows the <sup>13</sup>C NMR spectra of oleic acid (OASM) and OA-5-90C oligomerized sample. The first peak was from the methyl group and appeared at 14 ppm in both OASM and OA-5-70C oligomerized sample. In addition, peaks assigned with the letter (b) at around 22- 35 ppm indicated the CH<sub>2</sub> of the oleic acid chain. Moreover, peak at 130 ppm corresponded to the olefinic carbons. In addition, the distinguishable peak for the CH methine carbon from estolides structure appeared at 74.1 ppm.<sup>24</sup> Also, a peak at 181 ppm indicated a carbonyl group from a carboxylic acid. Finally, two different carbonyl groups, at around 173.8 ppm and 180 ppm indicated an ester estolides and carbonyl from a carboxylic acid, respectively.<sup>25</sup>



**Figure 20.**  $^{13}\text{C}$  NMR spectra of (a) OA starting material (b) OA-5-90C oligomerized sample

Figure 21 shows the  $^{13}\text{C}$  NMR spectrum of OA-5-130C. The peak at 74 ppm disappeared which corresponds to estolides structure. Also, the intensities of the peaks reduced due to the oligomerization of the OA and the amount of the estolides and lactones reduced. In addition, the double bond at 130 ppm did not appear due to the oligomerization of the double bond.

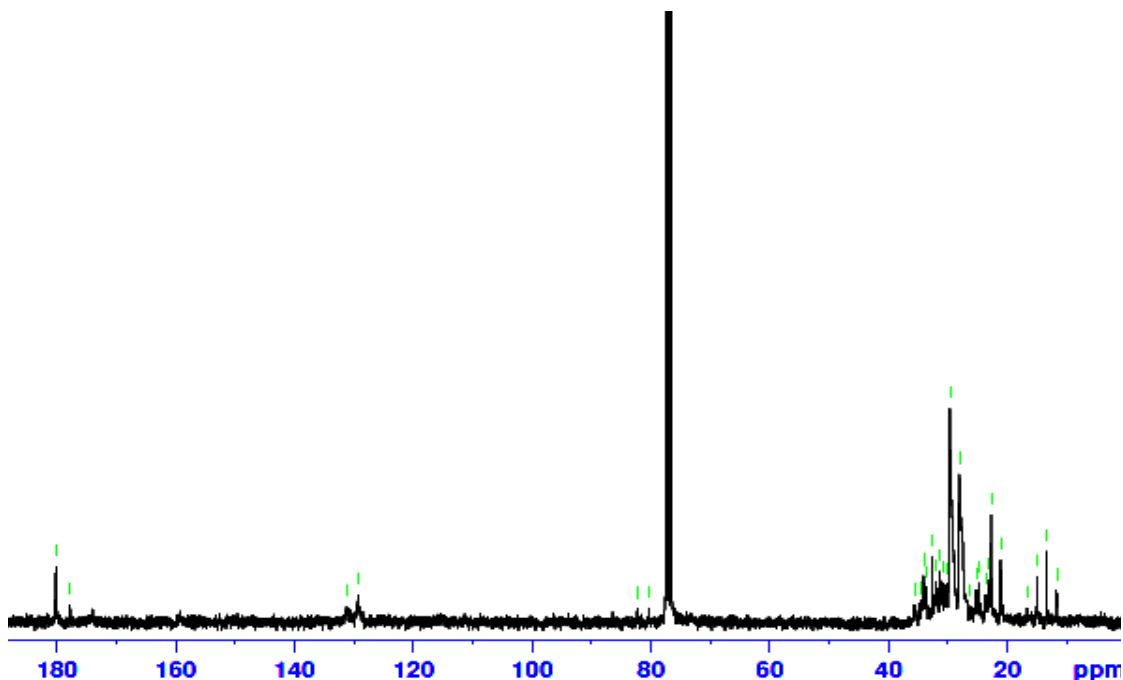


Figure 21.  $^{13}\text{C}$  NMR spectrum of OA-5-130C oligomerized sample

Table 14 shows the acidic value of MS and OA samples. The acid value of MS-5-70C, MS-5-90C, and MS-5-110C increased with increasing oligomerization temperatures. In addition, the acid value of MS-5-130C decreased due to the oligomerization of the sample and may be due to a low molecular weight compound. Moreover, the acid value of OASM decreased from 202 mg KOH/g to 133 mg KOH/g in MS-5-90C oligomerized sample and increased in OA-5-110C and OA-5-130C oligomerized samples because the formation of estolides and lactones decreased.

Table 14 shows the iodine value for the fatty acid and the fatty acid methyl ester. The iodine value of MS-5-70C, MS-5-90C, MS-5-110C, and MS-5-130C oligomerized samples decreased with increasing temperatures. In addition, the iodine value of OA-5-70C, and OA-5-90C oligomerized samples decreased while, OA-5-110C, and OA-5-130C increased with increasing temperatures.

**Table 14. Acid value and Iodine value of MS and OA samples**

Sample	Acid value (mg KOH/g)	Iodine value (g I <sub>2</sub> / 100g)
MSSM	2	143
MS-5-70C	18	120
MS-5-90C	30	113
MS-5-110C	30	115
MS-5-130C	27	110
OASM	202	90
OA-5-70C	142	49
OA-5-90C	133	46
OA-5-110C	142	53
OA-5-130C	141	60

Table 15 shows the yield of estolides yields determined from the <sup>1</sup>H NMR spectra of OA-5-70C, OA-5-90C, OA-5-110C, and OA-5-130C oligomerized samples by comparing the area under the peaks of CH<sub>3</sub> and CH linkage of estolides. The amount of estolides decreased with increasing temperatures.

**Table 15. Estolides yield of Oleic Acid**

Sample	Estolides (%)
OA-5-70C	28
OA-5-90C	22
OA-5-110C	17
OA-5-130C	-

## Chapter IV

### 4. Conclusions:

The objective of this work was to examine cationic oligomerization of vegetable oils with a superacid initiator. Cationic oligomerization of methyl soyate and oleic acid was carried out with a superacid (tetrafluoroboric acid) as the catalyst. The effects of catalyst concentration and temperature were studied.

The oleic acid oligomerization yielded lactones and estolides. Once the reactions were completed, the materials were characterized by GPC, IR, and  $^1\text{H}$  and  $^{13}\text{C}$  NMR. Increasing the concentration of the catalyst increased the formation of dimer and other oligomers with methyl soyate, while, OA showed formation of estolides and lactones. In addition, increasing the oligomerization temperature of MS increased the formation of dimers and other oligomers, while, OA showed a decrease in the formation of estolides and lactones.

The oligomers in MS and OA oligomerized samples were increased with temperature and it has been shown that temperature plays an important part in the regioselectivity of formation lactones and estolides.<sup>23</sup> The spectra of IR of MS samples showed noticeable peaks that indicated FAMEs products, while IR for oleic acid samples had obvious peaks corresponding to estolides and lactones products. Decreasing the double bonds absorption peak, the OH broad peak, and the multiple carbonyl peaks at OA-5-130C was consistent with the formation of estolides and lactones.

$^1\text{H}$  and  $^{13}\text{C}$  NMR for MS samples and oleic acid samples gave signals which were consistent with the formation of lactones and estolides. Especially for oleic acid which showed a methine carbon at 74 ppm and two carbonyl groups at around 173.8 indicated to an ester carbonyl and at around 180 ppm indicated to carboxylic acid groups. Moreover, the peak at 4.8 ppm indicated a linkage due to an estolides and the small peaks at 2.5 ppm, 4.2 ppm, and 4.5 ppm were consistent with estolide and lactones formation.



## References

1. Ronda, J. C.; Lligadas, G.; Galià, M.; Cádiz, V. Vegetable oils as platform chemicals for polymer synthesis. *European Journal of Lipid Science and Technology*, **2011**, *113*(1), 46–58.
2. Demirbaş, A. Biodiesel fuels from vegetable oils via catalytic and non-catalytic supercritical alcohol transesterifications and other methods: a survey. *Energy Conversion and Management*, **2003**, *44*(13), 2093–2109.
3. Gunstone, F. D. *Vegetable Oils in Food Technology: Composition, Properties, and Uses*. Blackwell Publishing Ltd: Boca Raton, FL 2002.
4. Hilditch, T. Triglyceride fats in human nutrition. *Proceedings of the Nutrition Society*, **1949**, *55*, 347-354.
5. Dutton N.J. History of the Development of Soy Oil for Edible Uses. *The Journal of the American Oil Chemists' Society*, **1981**, *58*(3), 234-236.
6. Odetoye, T.E.; Ogunniyi, D.S.; Olatunji G.A. Vegetable oil as industrial raw material, *Chemical Society of Nigeria*, **2008**, 74-79.
7. Grain. Corporate power: The palm-oil biodiesel. Seedling. **2007**. Web 8 Dec. 2013, <http://www.grain.org/article/entries/611-corporate-power-the-palm-oil-biodieselne>
8. Moss, G.; Smith, P.; and Tavernier, D. Glossary of class names of organic compounds and reactive intermediates based on structure. *Pure and Applied Chemistry*, **1995**, *67*, 1307–1375.

9. Hilditch, T., Williams N. *The chemical constitution of natural fats*. Chapman & Hall, London 1964.
10. Firestone, D. Determination of the iodine value of oils and fats: summary of collaborative study. *Journal of the Association of Official Analytical Chemists International*, **1994**, 77(3) 674-6.
11. Koleske, J. *Paint and Coating Testing Manual*. 13 ed, American Society for Testing and Materials: Philadelphia, PA 1995.
12. Alemdar, N.; Erciyas, T.; Bicak, N. Production of oil-based binder by RAFT polymerization technique. *Progress in Organic Coatings*, **2010**, 69, 522–526.
13. Jenkins, A.; Kratochvil, P.; Stepto, R.; and Suter, U. Glossary of basic terms in polymer science. *Pure and Applied Chemistry*, **1996**, 68, 2287–2311.
14. Petrović, Z. Polymers from Biological Oils. *Contemporary Materials*, **2010**, 1(1), 39–50.
15. Ionescu, M.; Petrovic, Z. In *Soybean - Applications and Technology*; Ng, T., Ed.; InTech: Rijeka, Croatia, 2011.
16. Ionescu M, Petrović S. Z. *Cationic polymerization of biological oils with superacid catalysts*, (2007) US Patent 7501479
17. Liu Z.; Sharma B.K.; Erhan S.Z. From Oligomers to Molecular Giants of Soybean Oil in Supercritical Carbon Dioxide Medium: 1. Preparation of Polymers with Lower Molecular Weight from Soybean Oil. *Biomacromolecules*, **2007**, 8(1), 233-239.

18. Larock, R.C.; Hanson, M., Li, F. *Lewis acid-catalyzed polymerization of biological oils and resulting polymeric materials*, (2001) The US patent 20020095007
19. . Burg, D.A.; Kleiman, R. Preparation of Meadowfoam Dimer Acids and Dimer Esters, and Their Use as Lubricants. *Journal of the American Oil Chemists' Society*, **1991**, 68(8), 600-603.
20. Biswas, A.; Sharma, B.; Willett, J.; Erhan S.; Cheng, H. Room-temperature self-curing ene reactions involving soybean oil. *Green Chemistry*, **2008**, 10, 290-295.
21. Nieto, R. New polyurethanes from vegetable oil-based polyols, Universitat Rovira i Virgili, **2011**, pp. 1–197.
22. Knothe, G.; Kenar, J. Determination of the fatty acid profile by  $^1\text{H-NMR}$  spectroscopy. *European Journal of Lipid Science and Technology*, **2004**, 106, 88–96.
23. Cermak, S.; Isbell, T. Synthesis of  $\delta$ -Stearolactone from Oleic Acid. *Journal of the American Oil Chemists Society*, **2000**, 77(3), 243–248.
24. Isbell, T.; Kleiman, R. Characterization of Estolides Produced from the Acid Catalyzed Condensation of Oleic Acid. *Journal of the American Oil Chemists' Society*, **1994**, 71(4), 1-5.
25. Cermak, S.; Isbell, T. Synthesis of Estolides from Oleic and Saturated Fatty Acids. *Journal of the American Oil Chemists' Society*, **2001**, 78(6), 557-565.

## **Appendix**

## Supplemental List

<b>Figure A</b>	<b>(a) <sup>1</sup>H NMR and (b) <sup>13</sup>C NMR spectra of MS-1 oligomerized sample</b>	<b>45</b>
<b>Figure B</b>	<b>(a) <sup>1</sup>H NMR and (b) <sup>13</sup>C NMR spectra of MS-3 oligomerized sample</b>	<b>46</b>
<b>Figure C</b>	<b>(a) <sup>1</sup>H NMR and (b) <sup>13</sup>C NMR spectra of OA-1 oligomerized sample</b>	<b>47</b>
<b>Figure D</b>	<b>(a) <sup>1</sup>H NMR and (b) <sup>13</sup>C NMR spectra of OA-3 oligomerized sample</b>	<b>48</b>
<b>Figure E</b>	<b><sup>1</sup>H NMR spectrum of MS-5-70 oligomerized sample</b>	<b>49</b>
<b>Figure F</b>	<b><sup>13</sup>C NMR spectrum of MS-5-70 oligomerized sample</b>	<b>49</b>
<b>Figure G</b>	<b><sup>1</sup>H NMR spectrum of MS-5-110C oligomerized sample</b>	<b>50</b>
<b>Figure H</b>	<b><sup>13</sup>C NMR spectrum of MS-5-110C oligomerized sample</b>	<b>50</b>
<b>Figure I</b>	<b><sup>1</sup>H NMR spectrum of MS-5-130C oligomerized sample</b>	<b>51</b>
<b>Figure J</b>	<b><sup>13</sup>C NMR spectrum of MS-5-130C oligomerized sample</b>	<b>51</b>
<b>Figure K</b>	<b><sup>1</sup>H NMR spectrum of OA-5-70C oligomerized sample</b>	<b>52</b>
<b>Figure L</b>	<b><sup>13</sup>C NMR spectrum of OA-5-70C oligomerized sample</b>	<b>52</b>
<b>Figure M</b>	<b><sup>1</sup>H NMR spectrum of OA-5-110C oligomerized sample</b>	<b>53</b>
<b>Figure N</b>	<b><sup>13</sup>C NMR spectrum of OA-5-110C oligomerized sample</b>	<b>53</b>

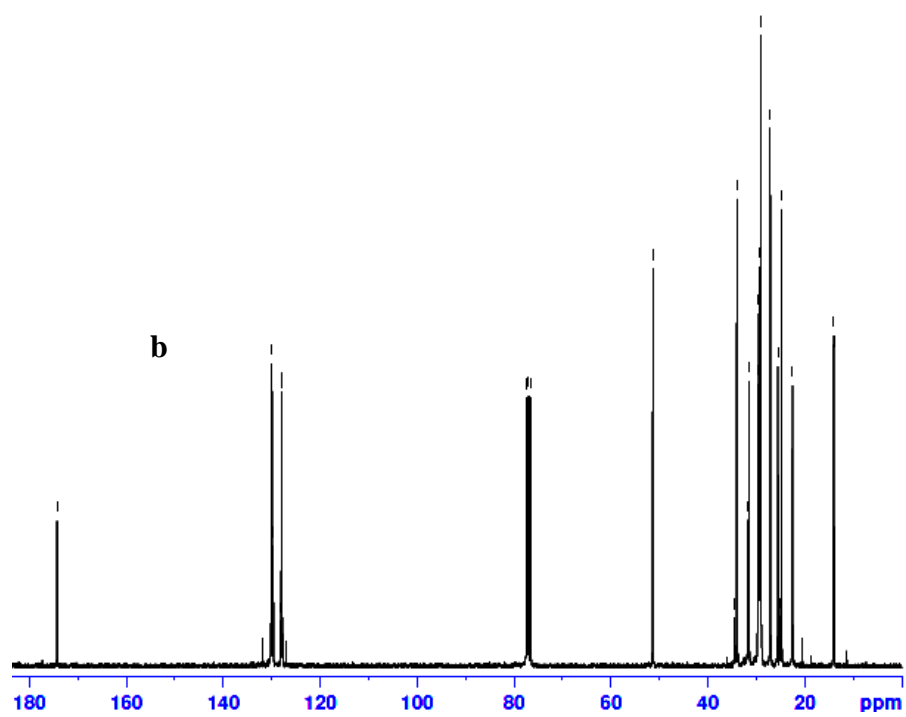
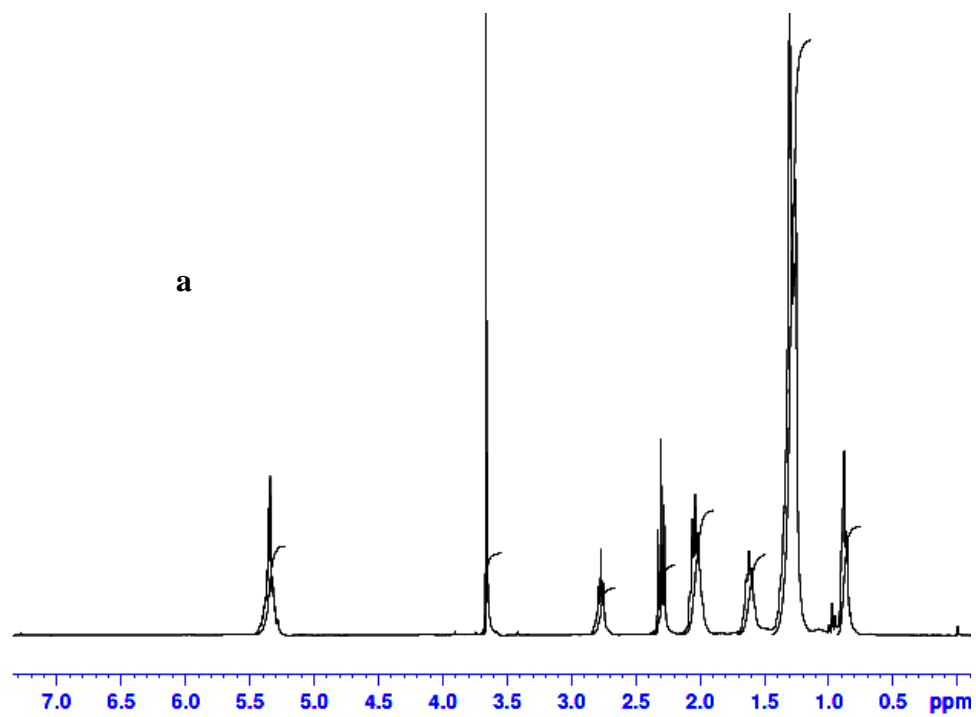
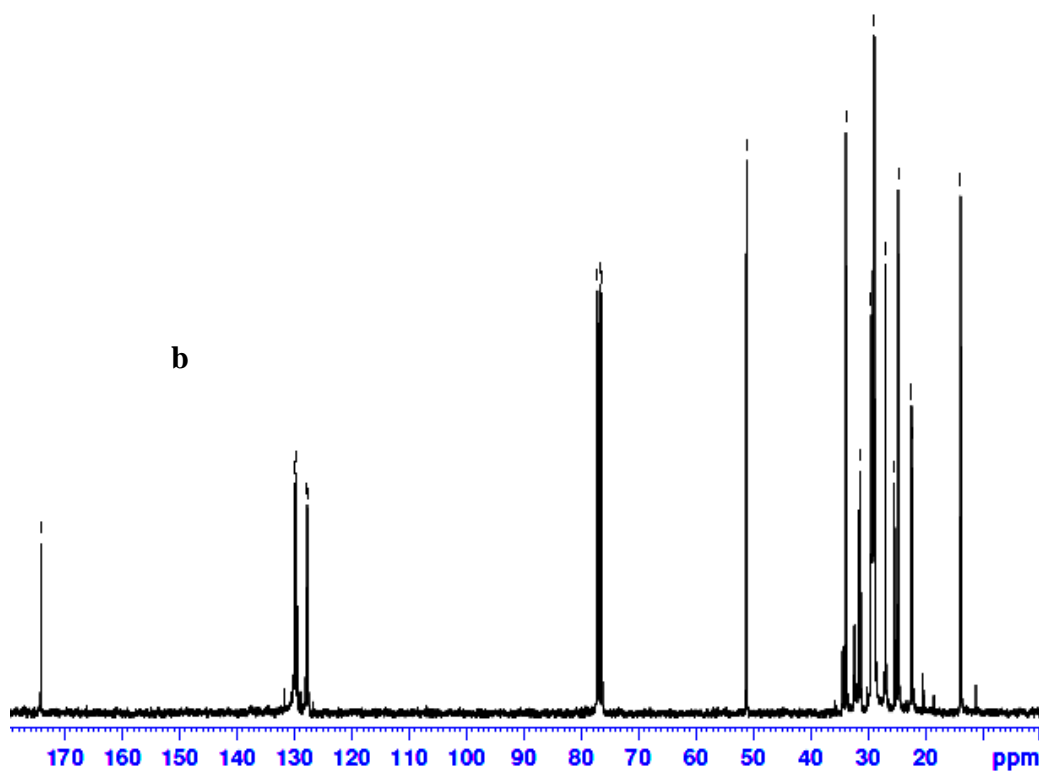
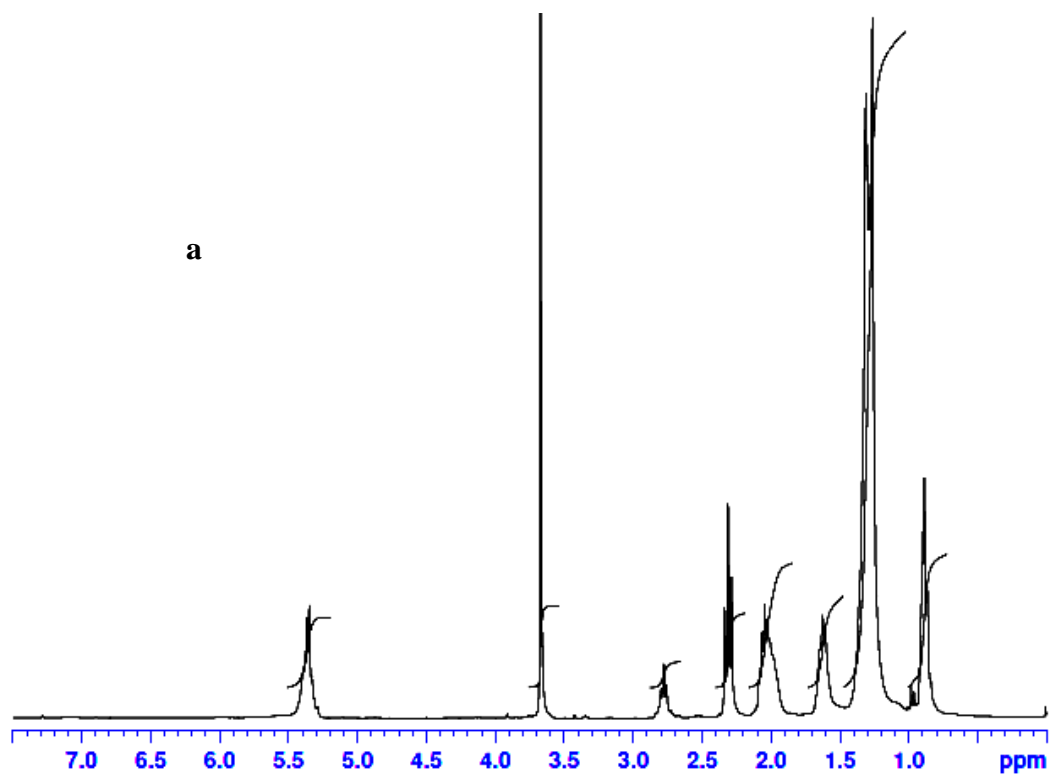


Figure A. (a)  $^1\text{H}$  NMR and (b)  $^{13}\text{C}$  NMR spectra of MS-1 oligomerized sample



**Figure B. (a)  $^1\text{H}$  NMR and (b)  $^{13}\text{C}$  NMR spectra of MS-3 oligomerized sample**

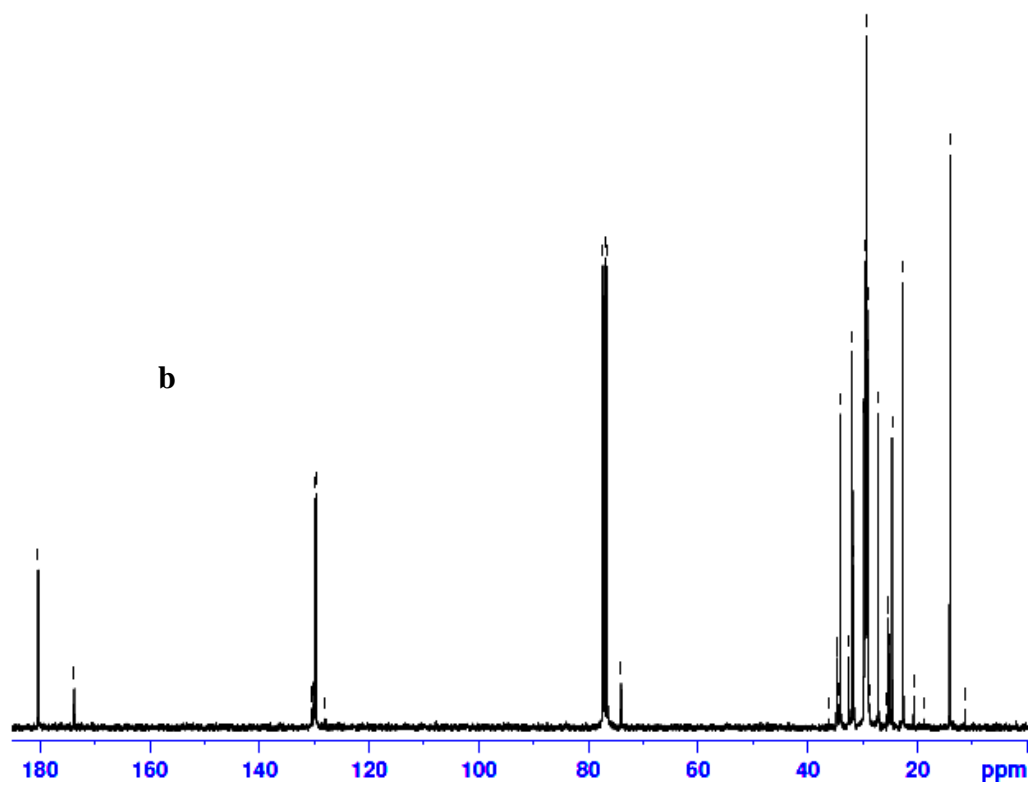
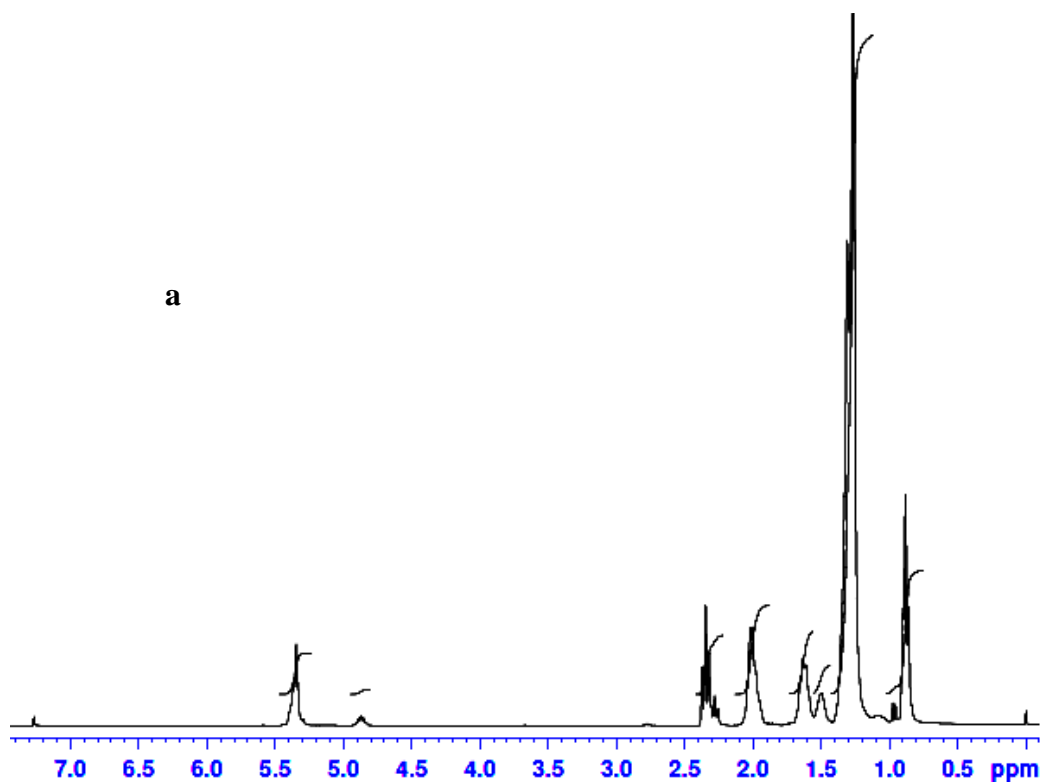


Figure C. (a)  $^1\text{H}$  NMR and (b)  $^{13}\text{C}$  NMR spectra of OA-1 oligomerized sample



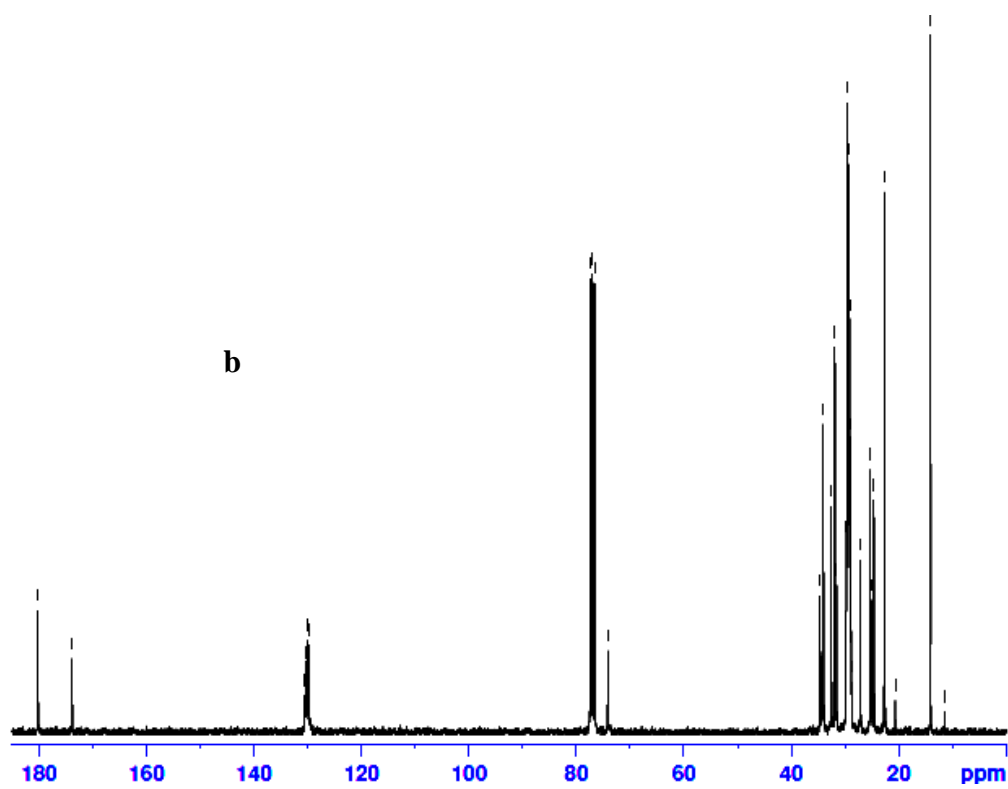
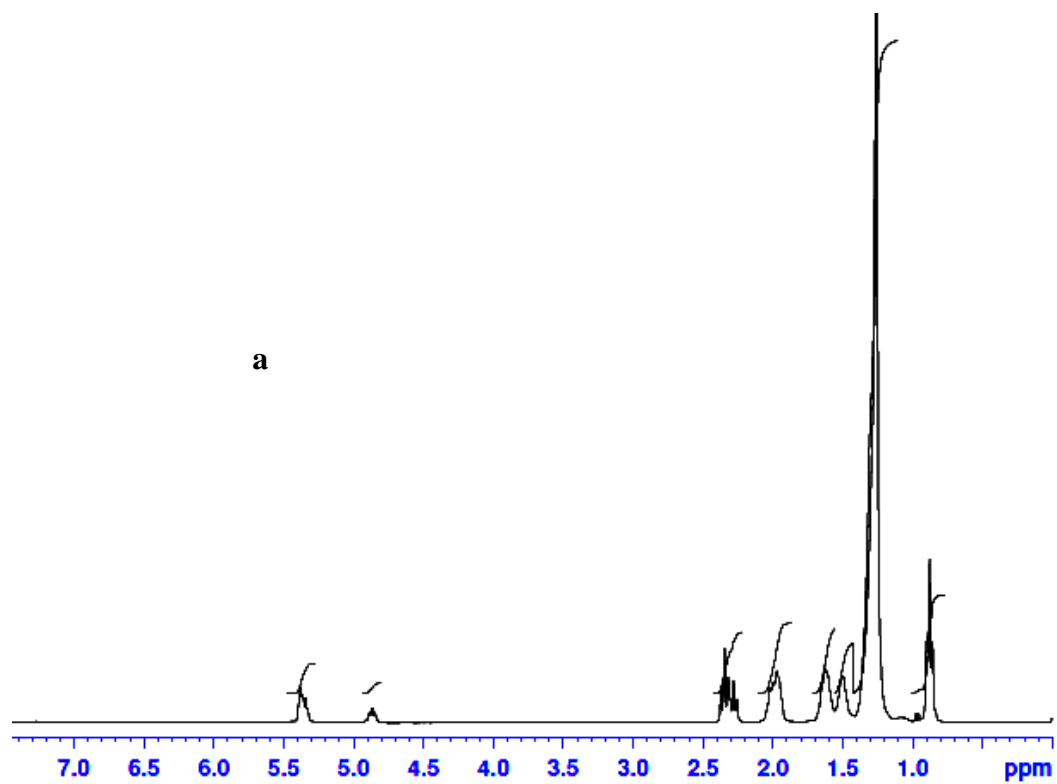


Figure D. (a)  $^1\text{H}$  NMR and (b)  $^{13}\text{C}$  NMR spectra of OA-3 oligomerized sample

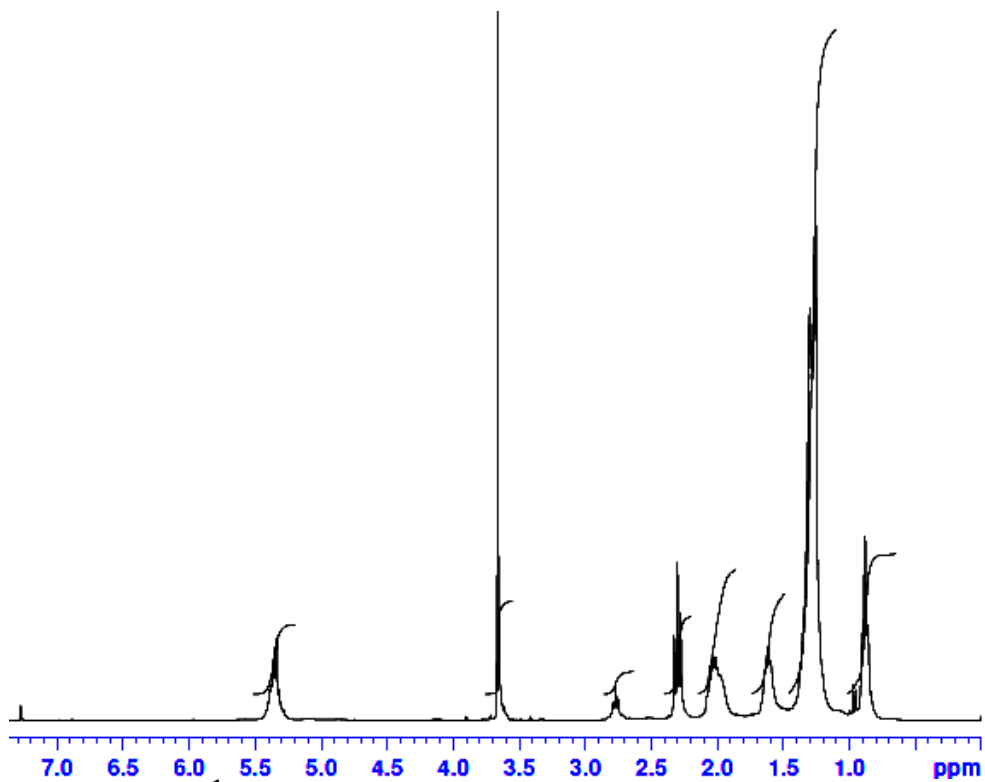


Figure E.  $^1\text{H}$  NMR spectrum of MS-5-70 oligomerized sample

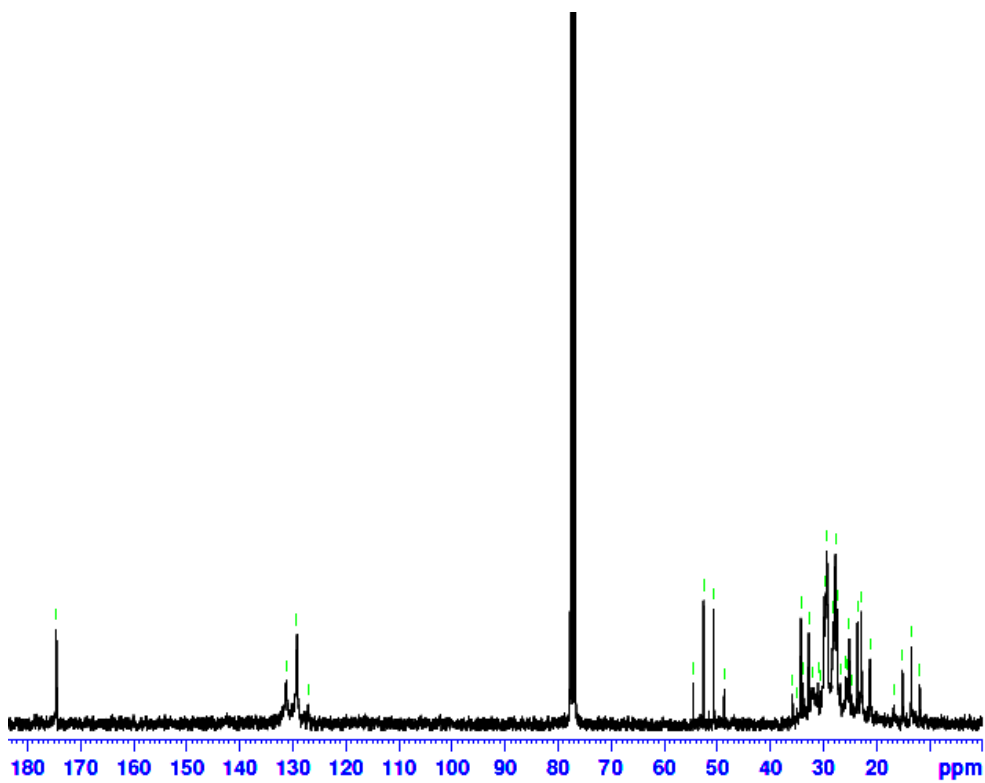


Figure F.  $^{13}\text{C}$  NMR spectrum of MS-5-70 oligomerized sample

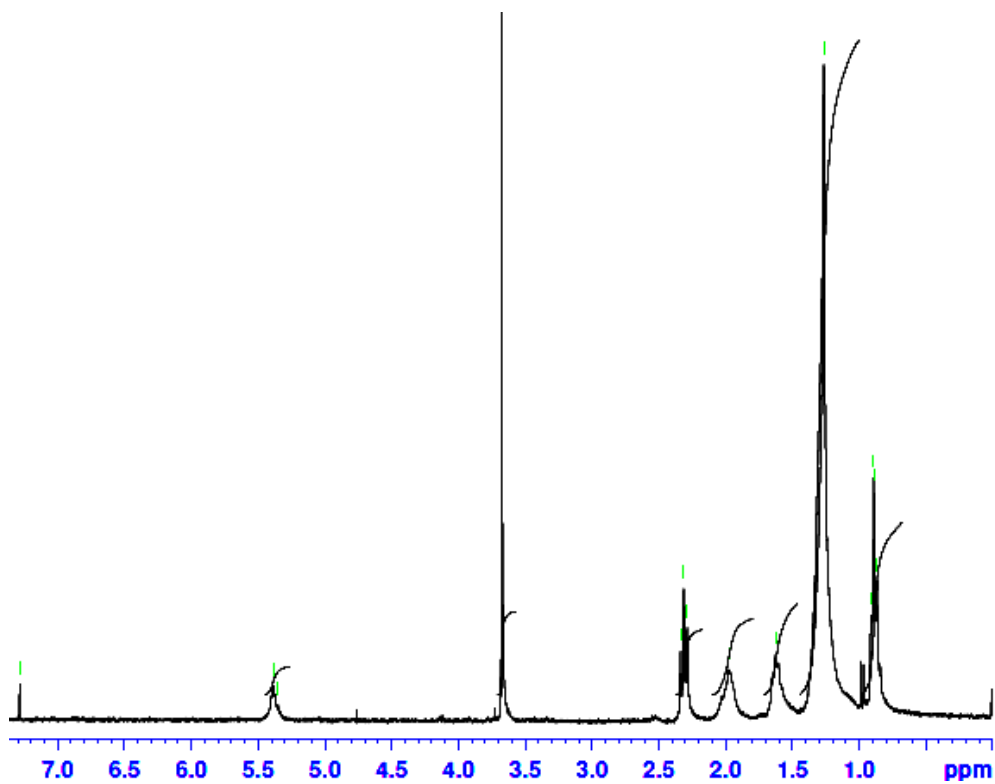


Figure G.  $^1\text{H}$  NMR spectrum of MS-5-110C oligomerized sample

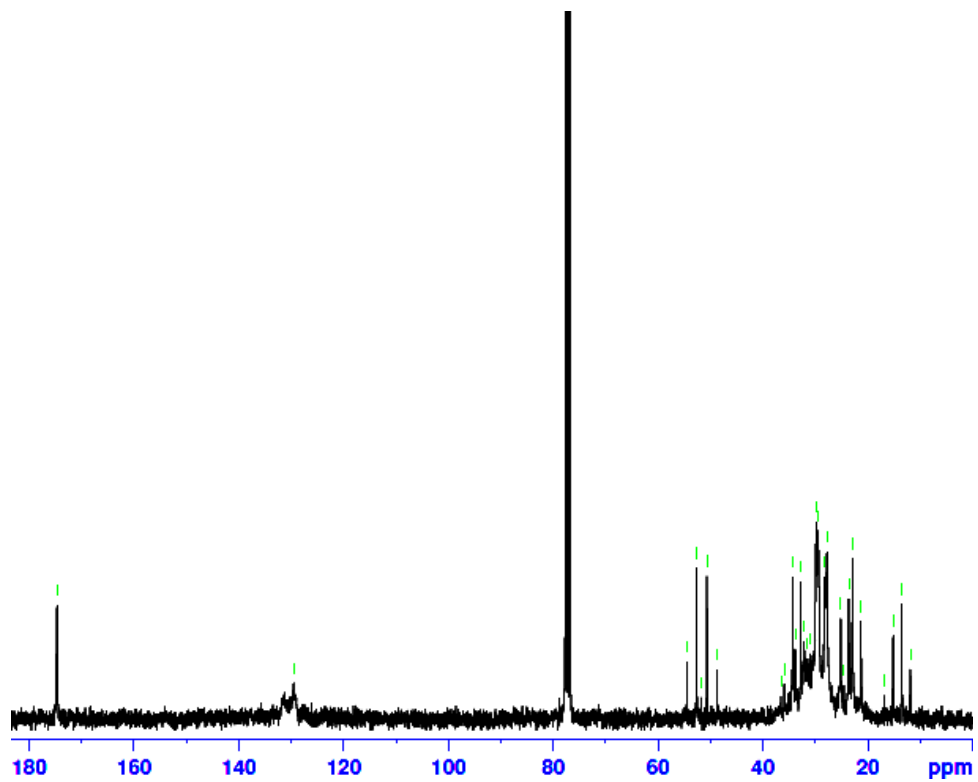


Figure H.  $^{13}\text{C}$  NMR spectrum of MS-5-110C oligomerized sample

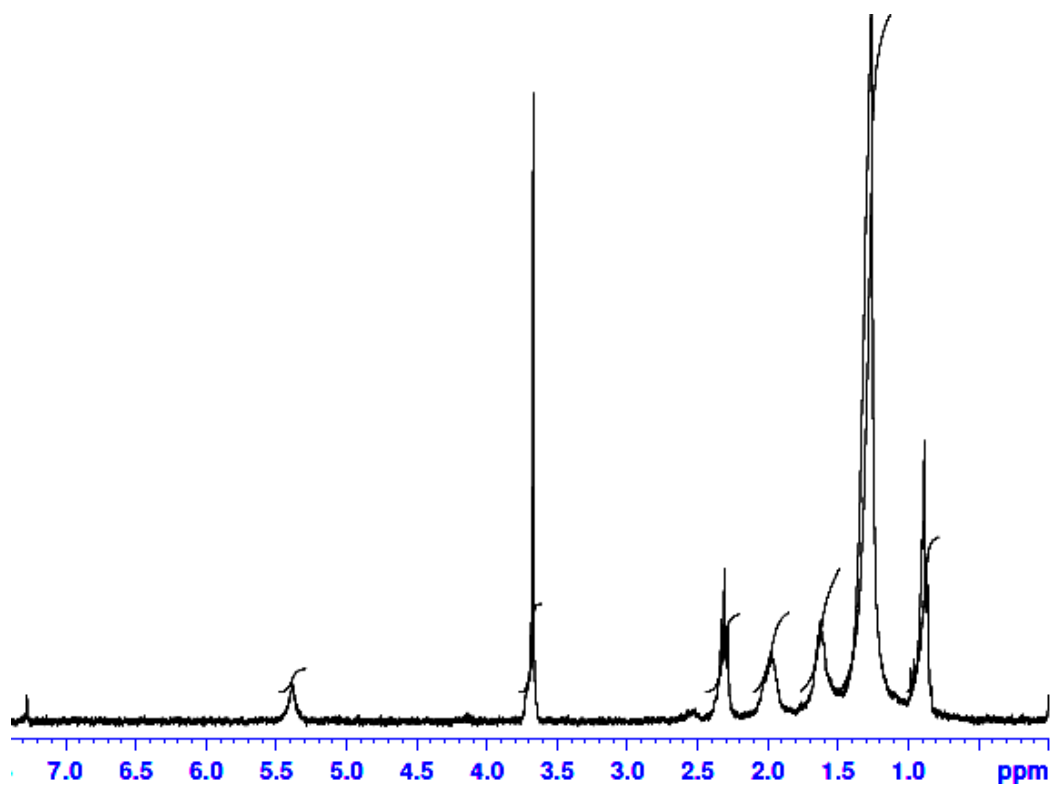


Figure I. <sup>1</sup>H NMR spectrum of MS-5-130C oligomerized sample

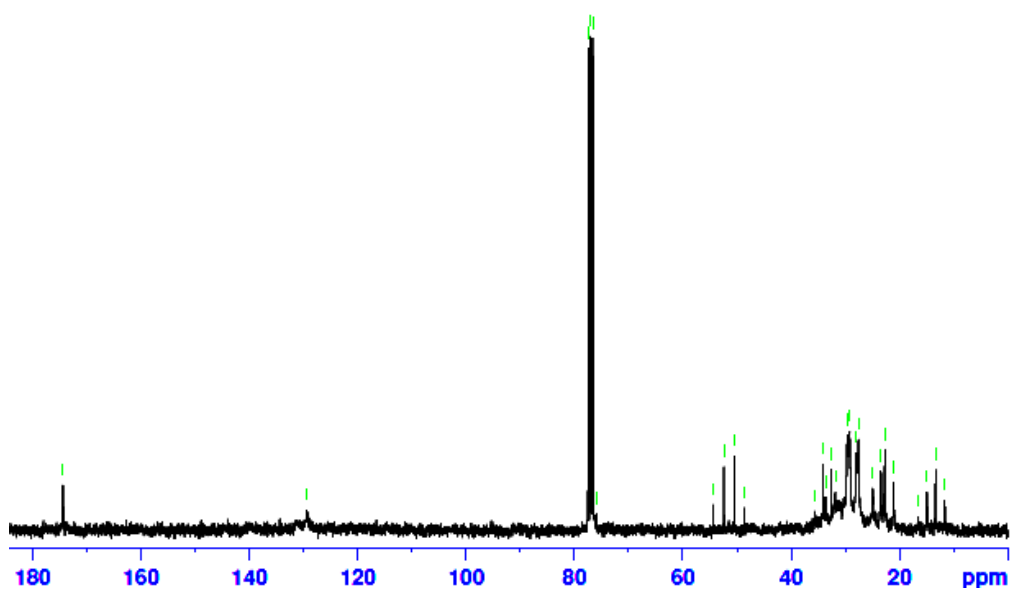


Figure J. <sup>13</sup>C NMR spectrum of MS-5-130C oligomerized sample

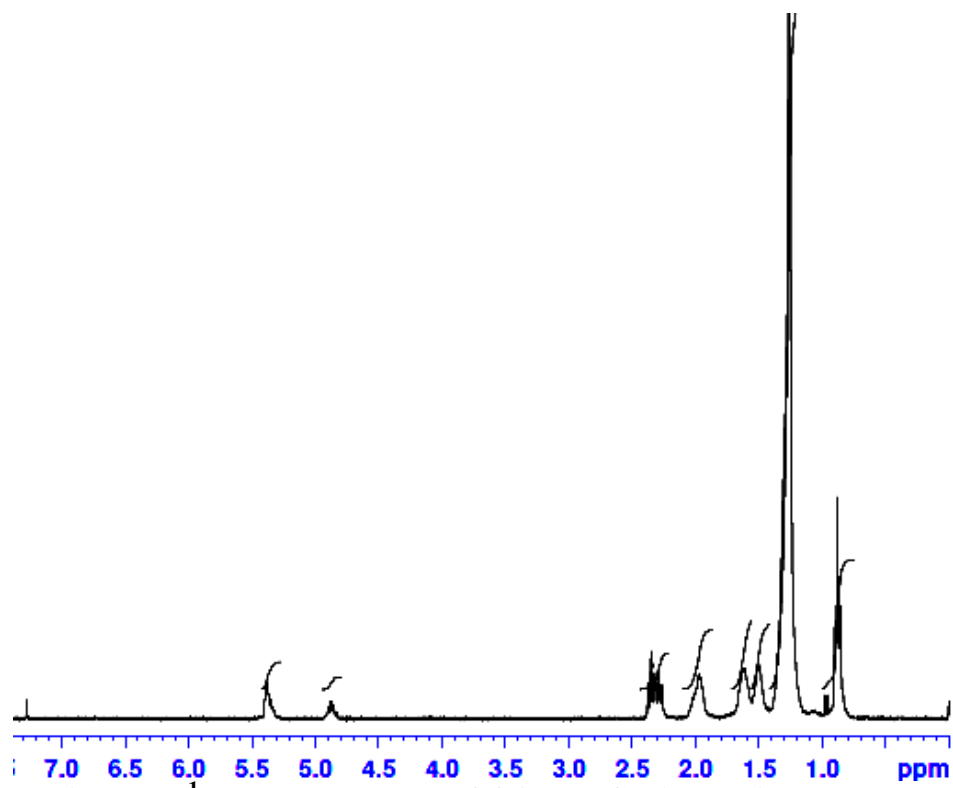


Figure K. <sup>1</sup>H NMR spectrum of OA-5-70C oligomerized sample

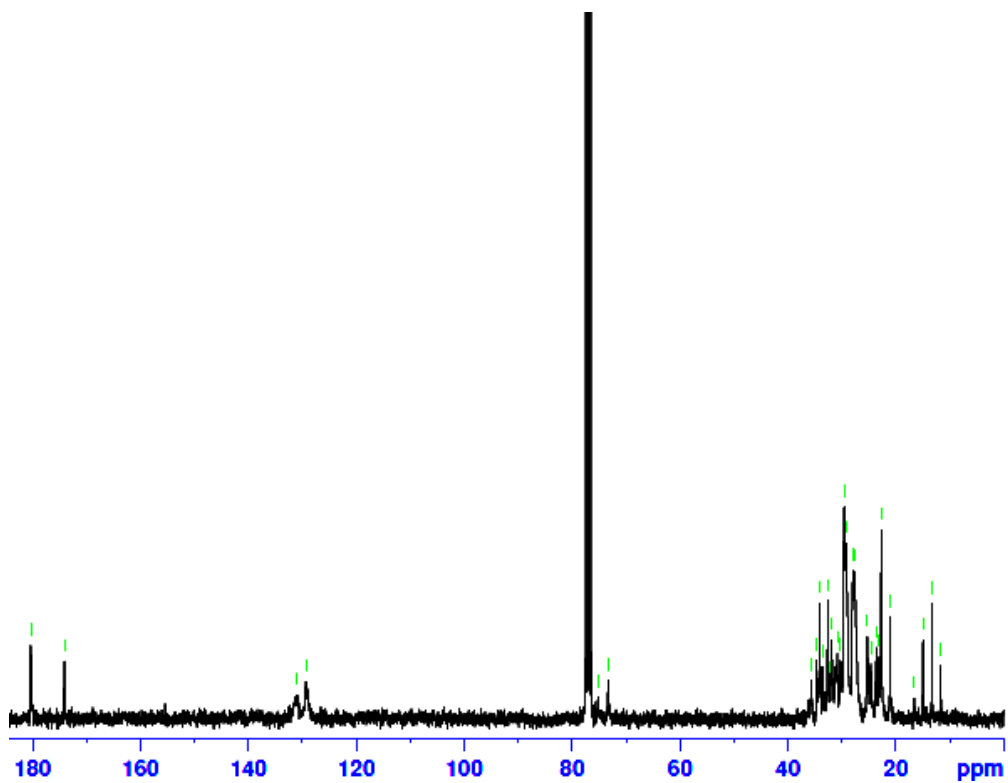


Figure L. <sup>13</sup>C NMR spectrum of OA-5-70C oligomerized sample

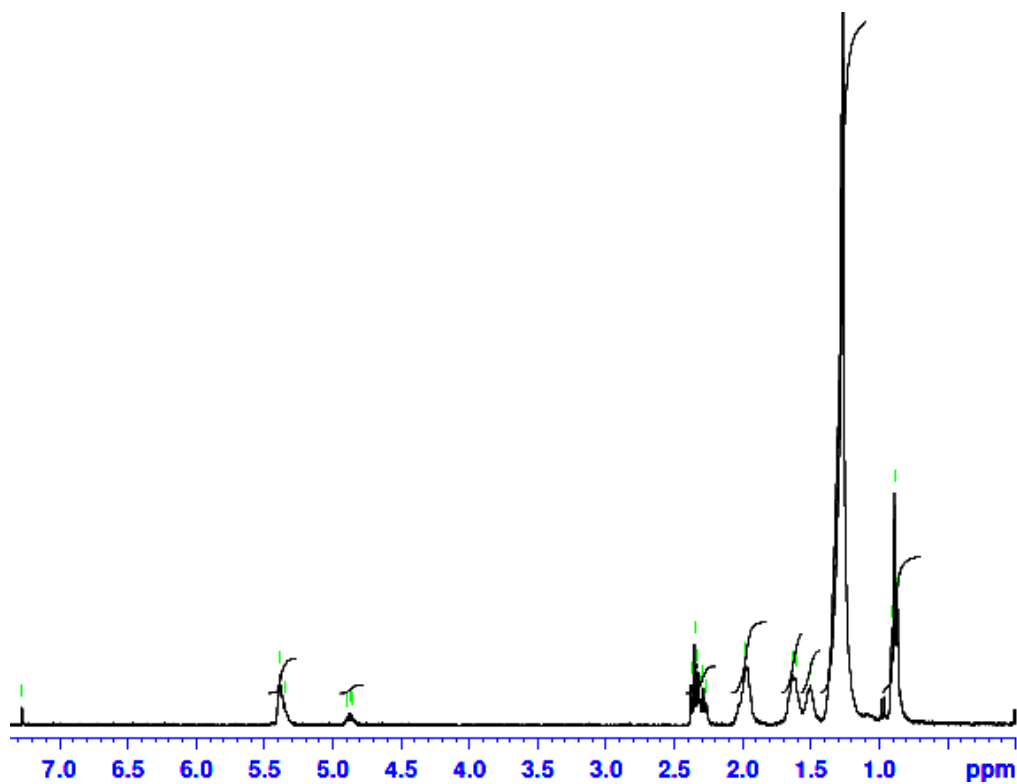


Figure M.  $^1\text{H}$  NMR spectrum of OA-5-110C oligomerized sample

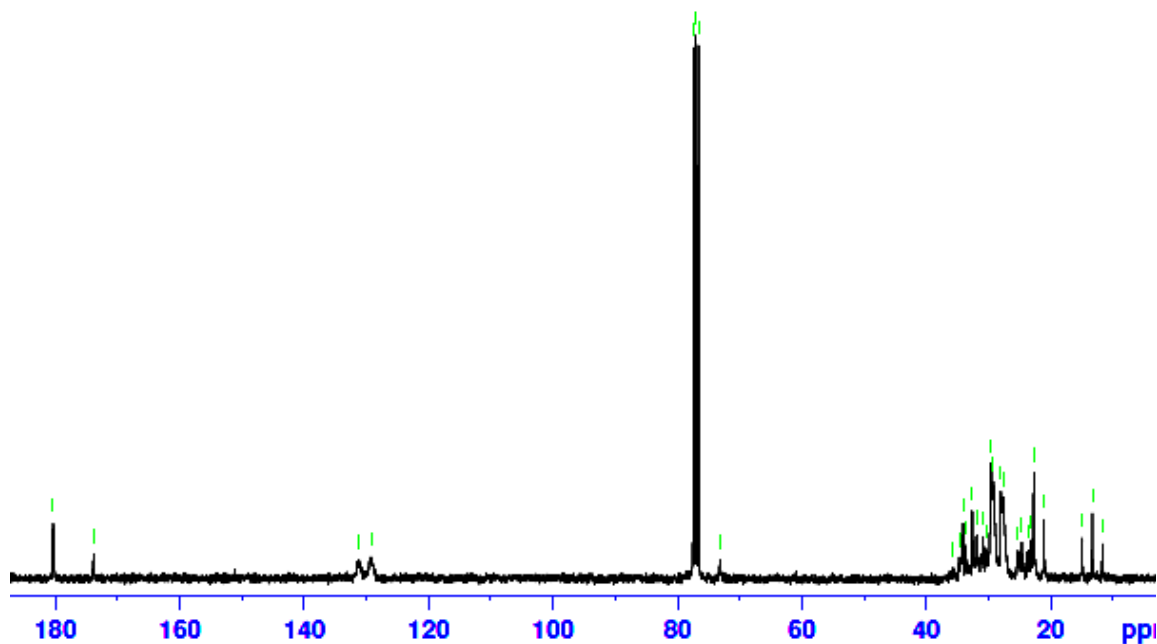


Figure N.  $^{13}\text{C}$  NMR spectrum of OA-5-110C oligomerized sample